6-4-2015

The Lifecycle of the Germinosome, a Bacillus subtilis Spore Germination Protein Complex

Anthony J. Troiano Jr
University of Connecticut - Storrs, atroiano@uchc.edu

The Lifecycle of the Germinosome,

a *Bacillus subtilis* Spore Germination Protein Complex

Anthony John Troiano Jr., Ph.D.

University of Connecticut, 2015

Fluorescent fusions to germination proteins of *Bacillus subtilis* were shown to colocalize into a single focus termed the germinosome in sporulating and germinating spores, but not in outgrowing spores. In sporulating cultures, fluorescent foci are seen immediately upon fluorescent signal detection, ~3 hours before dipicolinic acid uptake, and in fluorescent strains with *sspA-lacZ* fusions, nearly in parallel with the accumulation of β-galactosidase activity. Furthermore, GerD-GFP self-associated in germinant receptor (GR) null strains, as well as in wild-type *Bacillus subtilis,* and facilitated germinosome formation in live *Escherichia coli* when expressed with *gerAA-mCherry*. These findings suggest the germinosome is made in parallel with GerD and GR synthesis, and that GerD acts as a scaffold that facilitates the colocalization of the GRs in the germinosome. Conversely, we found that after initiation of spore germination, the germinosome foci

changed into larger disperse patterns, with ≥75% of spore populations displaying this pattern in spores germinated for 1 h, although >80% of spores germinated for 30 min retained foci. Western blot analysis revealed that levels of GR proteins and the SpoVA proteins changed minimally during this period, although GerD levels decreased ~ 50% within 15 min in germinated spores. Since the dispersion of the germinosome during germination was slower than the decrease in GerD levels, either germinosome stability is not compromised by ~ 2-fold decreases in GerD levels, or other factors such as restoration of rapid IM lipid mobility, are also significant in germinosome dispersion as spore germination proceeds. All of these data suggest that GerD, while important for facilitating the formation of the germinosome in sporulation, may not be as significant in maintaining this protein complex in actively germinating spore populations.

The Lifecycle of the Germinosome,

a *Bacillus subtilis* Spore Germination Protein Complex

Anthony John Troiano Jr.

B.S., University of New Hampshire, Durham, NH., USA, 2010

A Dissertation

Submitted in Partial Fulfillment of the

Requirements for the Degree of

Doctor of Philosophy

at the

University of Connecticut

2015

APPROVAL PAGE

Doctor of Philosophy Dissertation

The Lifecycle of the Germinosome,

a *Bacillus subtilis* Spore Germination Protein Complex

Presented by

Anthony J. Troiano Jr.

Major Advisor

_____

Peter Setlow

Associate Advisor

_____

Ann E. Cowan

Associate Advisor

_____

Ji Yu

Associate Advisor

_____

Lawrence Klobutcher

The University of Connecticut

2015

ACKNOWLEDGEMENTS

I first and foremost extend my sincerest thanks and gratitude to my advisor, Dr. Peter Setlow, for giving me the opportunity to work in his laboratory and for the dedication and guidance he has shown as a mentor. The work doctrine of this laboratory defines what science is meant to be, a collaborative and altruistic environment, and it has allowed me to grow both professionally and personally. Peter's sense of humor, albeit one speed set to sarcasm, brought levity to the long days, and helped me through some very difficult times in my graduate career. I would also like to thank my associate advisors, Dr. Ann E. Cowan, Dr. Ji Yu, and Dr. Lawrence Klobutcher, for their hard work in helping me develop into the scientist I have become. Ann and Ji were invaluable assets in learning all things microscopy, and Larry's feedback during meetings, work in progress talks, and journal clubs was incredibly helpful, and is very appreciated.

I would like to extend my thanks to the MBB department office staff, Patricia Shultz and Bridget Clancey-Tenan, who continually make everything run smoothly in our department. A very special thanks to all of the faculty and students in the MBB program who contributed to my positive experience here at UCONN, I continue to believe we are one of the best and most diverse graduate school departments at the health center, which benefits students immensely with regards to journal club and work in progress feedback.

To the members of the Setlow lab, both past and present, thank you for making my experience here so positive and rewarding. To Dr. Barbara Setlow, words cannot express my thanks in everything you have helped me with, from any material or media I needed in the laboratory, to gardening advice, to being there to listen to me in general, I thank you so very much. You are the super glue that holds the Setlow Lab together

Barbara. To George Korza, our laboratory technician, you provided me with direction and troubleshooting advice nearly every day for four and a half years, you are an invaluable asset to the laboratory. Dr. Sonali Ghosh, Dr. Kerry-Ann Stewart, and Dr. Keren Griffiths, my fellow graduate students in the lab before me, thank you for being friends and amazing coworkers throughout my tenure at UCONN, and to Keren specifically, thank you for setting the foundation for my dissertation research in your discovery of the "germinosome."

Finally I would like to thank my close friends and most importantly my family for their love and support throughout my long and seemingly endless journey. To my parents Laurie and Tony, who never stopped supporting me in all my endeavors throughout my life, and to my Godparents, Vinny and Sharon, for their unwavering love and support in Connecticut, a very special thank you. My sister Kate and brother-in-law KJ, thank you both for your love and support, and letting me visit you down in St. Thomas whenever I needed a change of scenery, something I will always treasure. To my grandmother, thank you for everything that you have done for me, the list seems endless. To my brothers in spirit, Andy and Chris (and his better half Danielle), Frank, and the rest of the Cape Cod group, thank you for being such good friends to me throughout this process and always being there in an instant when I needed a helping hand or someone to vent to. Lastly, to my dear late friend Zach Hauser, losing you halfway through my graduate career was one of the hardest situations of my life, but I will always remember our wonderful friendship and look back on it with fond memories. It is truly remarkable to have so many special people in my life, and I thank you all deeply for your support these past five years.

TABLE OF CONTENTS

LIST OF TABLES

LIST OF FIGURES

CHAPTER 1

INTRODUCTION

1-1 The Life Cycle of *Bacillus subtilis*

Bacillus subtilis is a gram positive, nonpathogenic, naturally occurring soil microbe, and depending on environmental conditions may proceed through one of two distinct life cycles (Fig. 1-1). If nutrients are present, *B. subtilis* undergoes normal cell division, producing two daughter cells, and continues this cycle of vegetative growth, with a generation time as short as 25 minutes depending on nutrient levels. However, when faced with nutrient starvation, *B. subtilis* undergoes the process of sporulation, dividing asymmetrically, and producing a morphologically distinct endospore within the mother cell, which is ultimately released into the environment. The released spore is resistant to a variety of stresses (heat, desiccation, radiation, toxic chemicals) and is metabolically dormant, a state in which it can remain for long periods of time.

Once environmental conditions become favorable, the dormant spore returns back to a metabolically active vegetative cell through the process of germination. This process of germination can be separated in two stages. In Stage I, upon initiation of spore germination spores will release some monovalent cations and the calcium chelate of pyridine-2, 6-dicarboxylic (dipicolinic acid [DPA]) (84,87). The spore core begins to take in water and swell, while the spore starts to lose some of its resistance properties. Stage II is characterized by further loss of resistance properties, hydrolysis of the peptidoglycan cortex (PG) layer, expansion of the inner spore membrane (IM), restoration of lipid mobility in the inner membrane, further core hydration, and loss of dormancy. Following Stage II germination, the spore begins outgrowth back into a vegetative cell, shedding its spore coat, resuming DNA, RNA, and protein synthesis, that all ultimately lead to cell growth and cell division.

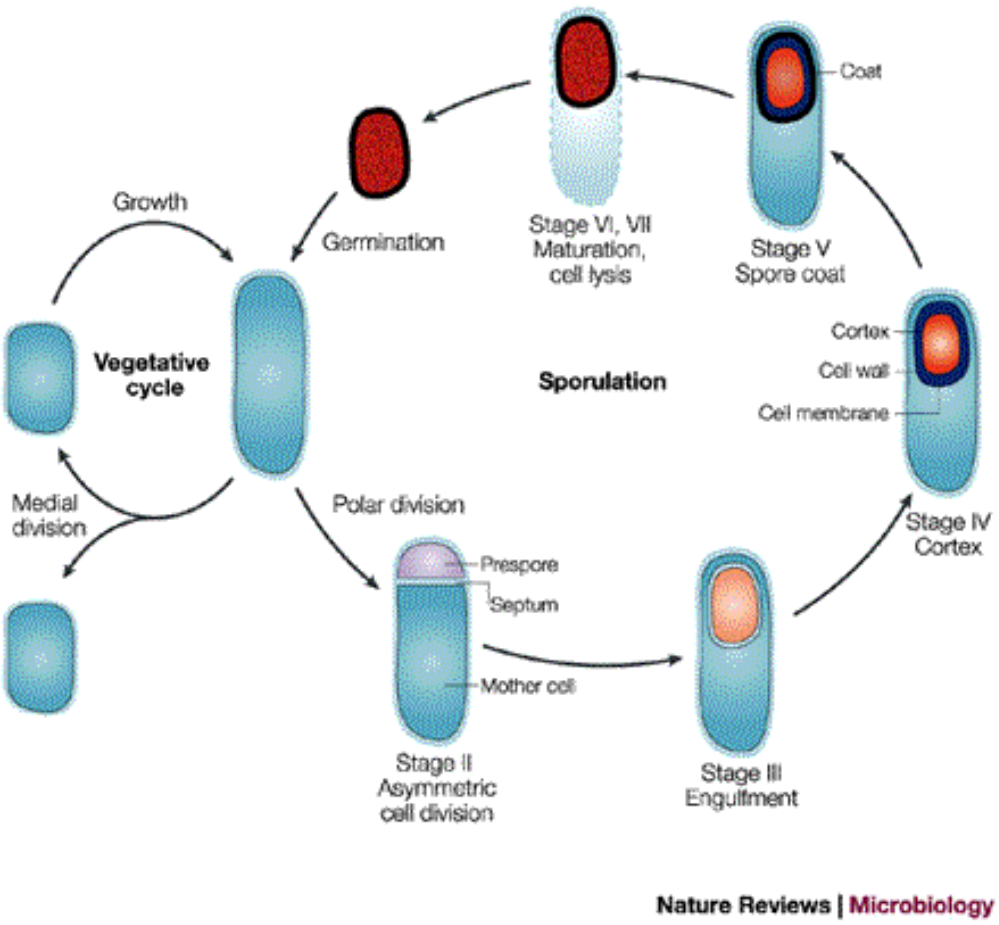

FIGURE 1-1 The life cycle of *Bacillus subtilis* (22). When nutrients are present *B. subtilis* undergoes regular vegetative growth and cell division, but when faced with starvation, begins the multistep process of sporulation. Beginning with an asymmetric cell division, the developing forespore is enclosed by the mother cell that deposits the spore coat onto the developing spore and ultimately lyses. The developing endospore matures into a dormant spore and is released into the environment where it remains dormant until favorable environmental conditions arise, beginning the process of germination and ultimately turning back into a vegetative cell.

1-2 The Spore Structure

Spores of *B. subtilis* are complex, multilayered structures and their resistance and dormancy are in part due to their unique structure. A cartoon representation depicting the many layers of the *Bacillus* species spore is shown in Figure 1-2 (88). Spores have several layers not found in growing cells including the outermost exosporium in some species, the coat, a layer in between the coat and exosporium termed the interspace, the outer membrane (OM), the PG cortex and PG germ cell wall, the IM, and finally the spore core. Each of these layers and their important features are discussed in the section below.

The outer most layer of the spore is the exosporium, a layer not present in *B. subtilis* spores, but pathogenic *Bacilli* species such as *B. anthracis* and *B. thuringiensis* as well as spores formed by many of the related *Clostridiales* order do contain an exosporium (3). The exosporium is a multilayered structure that has different patterns that vary among species, and may act as a semi permeable barrier that protects the developing spore (3,32). Synthesized concurrently with the spore coat, the exosporium is separated from the underlying coat by the interspace layer (32). The coat is the outermost known layer in *B. subtilis* and is deposited by the mother cell around the developing spore in sporulation (22). Composed of mainly protein (~30% total spore protein) (17,31), the total number of coat proteins is estimated to be >70 (40), which serve a protective function for the spore, providing resistance to lysozyme and some chemicals (17,32). The spore coat may be important for spore germination, as coat defective spores are impaired in their ability to germinate normally (28).

Underneath the spore coat lie two membranes, an OM, which is mother-cell derived and sits directly beneath the coat, and the IM, which is forespore derived. In between these two membranes are two layers, the PG cortex, and the germ cell wall. The exact role for the OM still remains unclear, and could be just a vestigial structure for the spore (32). Directly under the OM is the cortex, which is comprised of PG that in *B. subtilis* spores has 50% of the muramic acid residues present as muramic acid-δ-lactam (MAL). MAL is recognized by the cortex lytic enzymes (CLEs) that hydrolyze cortex PG, but not germ cell wall PG during spore germination (24). The cortex functions to maintain the inner spore core in its dehydrated state, an important factor that contributes to the spore's resistance properties (24).

Beneath the PG cortex is the germ-cell wall, a thin layer of highly cross-linked PG with a structure similar to that of vegetative cell wall PG, and which also lacks MAL (24). Under the germ cell wall is the IM, which serves as a major permeability barrier in dormant spores. Lipids in the IM are immobile (12), but during germination mobility is restored and the IM expands ~2 fold without any ATP synthesis or new membrane production (12). Within the IM are the nutrient germinant receptors (GR), which play a critical role in nutrient germination (36,59), as well as GerD, an accessory germination protein (65,66), all of which have been found to colocalize in dormant spores into a structure termed the "germinosome" (30,103).

The final layer of the spore is the core, which remains in a relatively dehydrated state until germination. Contained within the core are the DNA, ribosomes, and enzymes required during outgrowth for DNA replication, transcription, translation, and metabolism (61). The core has low water content (25-50% of wet weight), which

contributes to its wet heat resistance (85), and a large amount (~10% of total spore dry weight) of the spore-specific molecule DPA in a 1:1 chelate with divalent cations, mostly Ca^{2+} (CaDPA) (26). DPA is synthesized in the mother cell and most likely taken up into the forespore through a SpoVA protein channel late in sporulation (45). The minimal metabolic activity within the spore core can most likely be attributed to the low water content, and proteins appear to be immobile in the core (11). The DNA within the core shows incredible resistance to damage from ultraviolet radiation, free radicals, and other toxic chemicals due to the presence of small-acid-soluble proteins (SASP) that make up 5-15% of the total proteins within the spore core (83,86). These proteins are synthesized in late stage sporulation, after engulfment, and under the control of the same RNA polymerase sigma factor as the GRs (107) Early in outgrowth the SASP are degraded to supply the spore with amino acids for energy production and protein synthesis (83).

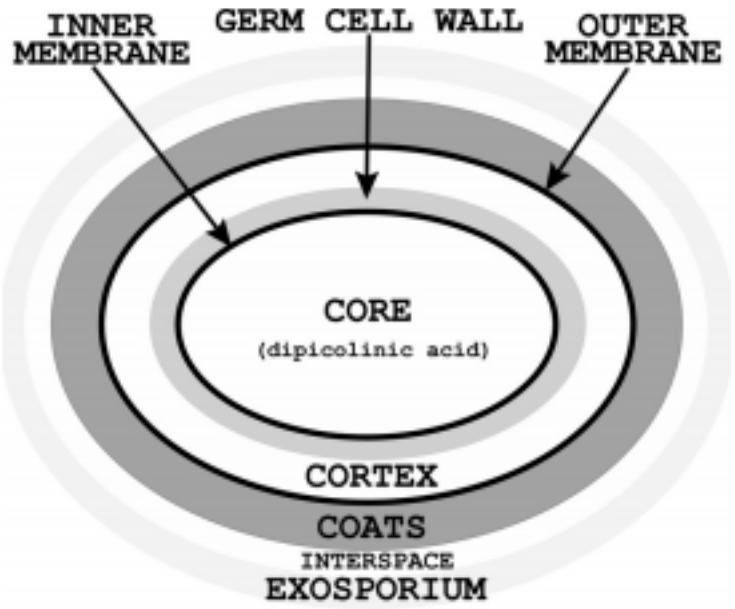

FIGURE 1-2 The structure of a *Bacillus* spore (88). The inner core contains a depot of CaDPA (~10% of spore dry weight), and is surrounded by an inner membrane that contains the GRs. This is followed by the germ-cell wall and a layer of unique PG called the cortex. Surrounding the cortex is an outer membrane derived from the mother cell and a proteinaceous coat layer sits on top of it. While *B. subtilis* does not contain an interspace layer or exosporium, other spore formers are encased in such layers.

1-3 Sporulation – Gene Regulation

When faced with nutrient starvation, *B. subtilis* initiates the process of sporulation in which a phosphorelay initiates the phosphorylation of Spo0A, a DNA binding protein that is the master regulator for the onset of sporulation. The extent of Spo0A phosphorylation determines a range of outcomes from biofilm production and cannibalism (when Spo0A is phosphorylated at lower levels) to sporulation (when Spo0A is phosphorylated at higher levels) (50). Spo0A directly regulates the transcription of ~120 genes as well as indirectly inducing several hundred other genes (25,54). Once sporulation is initiated, the mother cell and developing forespore undergo distinct developmental pathways, which are controlled by five different RNA polymerase sigma (σ) factors.

First, Spo0A activates σ^H, which controls gene expression of the *ftsAZ* operon that is essential for asymmetric division (34,54). The early sigma factors σ^F and σ^E are both produced under the Spo0A regulon prior to septum formation, but remain inactive until division is complete. In the forespore, σ^F is activated when the phosphatase SpoIIE activates the anti-anti sigma factor SpoIIAA after polar septum formation (20). Activated SpoIIAA draws the anti-sigma factor SpoIIAB away from σ^F, allowing σ^F to activate *sigG* and *spoIIR* expression (18). SpoIIR is secreted into the intermembrane space and activates a protease, SpoIIGA, which removes an inhibitory pro-peptide from σ^E in the mother cell. This criss-cross pattern of gene activation between mother cell and developing forespore is a hallmark of *B. subtilis* sporulation, as the sigma factors that control sporulation genes are sequentially and alternatively activated between the forespore and mother cell (Fig. 1-3).

In the mother cell, σ^E activation drives the transcription of several genes that encode a hydrolase complex mediating engulfment (1,19). This allows for assembly of a channel composed of components controlled by both forespore-specific σ^F and mother cell specific σ^E (79). This "feeding tube" bridges the mother cell and forespore compartments and is needed for σ^G activity in the forespore (6,16). Furthermore, σ^G is not activated until the completion of engulfment (77), and it auto-activates its own production (95). Both σ^G and σ^K control the transcription of genes in late stage sporulation, with σ^G being forespore specific and σ^K mother cell specific.

Like σ^F, σ^G is held in an inactive state by the anti-sigma factor SpoIIAB (107), but once engulfment is complete σ^E-dependent mother cell protein SpoIIIA triggers activation of σ^G (33,107). Like σ^E, σ^K is also synthesized as a pro-sigma factor, pro-σ^K (33,107), and is processed to the active σ^K form by *spoIVB*, which is under the transcriptional control of σ^G (16). This is a classic example of criss-cross sigma factor activity in sporulation between the mother cell and developing spore (Fig. 1-3). The genes transcribed by σ^G function to couple late prespore and mother cell gene expression, protect spore DNA, and prepare the spore for germination (33,107). Conversely, the primary function of genes transcribed by σ^K control formation of the spore coat and spore maturation, as well regulating σ^K dependent transcription (23,107).

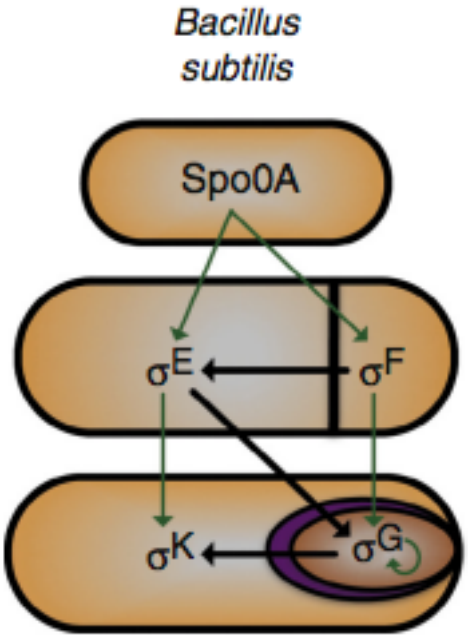

FIGURE 1-3 Sigma factor activity is regulated in "criss-cross" pattern in *Bacillus subtilis* (23). Activation of Spo0A allows for transcription of σ^E and σ^F, but it is not until after polar septum formation that σ^F becomes active in the forespore. Expression of the σ^F regulon leads to activation of σ^E in the mother cell. Products of the σ^F and σ^E regulon allow σ^G activity in the forespore, and σ^G auto-activates its production and induces σ^K activation in the mother cell. Both σ^E and σ^F are required for σ^G and σ^K activation in the forespore and mother cell, respectively.

1-4 Sporulation – Morphological Stages

As mentioned previously, during conditions of nutrient deprivation, *B. subtilis* initiates the process of sporulation. The end result of this process is a morphologically distinct cell type, the spore. Sporulation has many distinct processes, and because of the large energy investment required, is very tightly controlled, as described in the previous section. The morphological changes that occur during spore formation were first identified using electron microscopy and are defined as stages 0-VII, which are depicted in Figure 1-1 (22). Stage 0 is defined as vegetative growth, but upon nutrient starvation, an axial chromatin filament is formed, a hallmark characteristic of Stage I (33). This filament is due to the condensation and stretching of two copies of the chromosome along the long axis of the cell (33). As the asymmetric sporulation septum forms in Stage II, separating the cell into the larger mother cell and the forespore, the forespore initially contains only the origin-proximal one third of the chromosome (33). In order for sporulation to proceed, the distal two-thirds of the chromosome need to be translocated into the forespore, which is done by SpoIIIE, a large polytopic membrane protein in the FtsK family of DNA transporters (51).

During Stage III, the mother cell membrane moves and encircles the forespore, engulfing it and creating a free-floating object surrounded by two membranes, one derived from the mother cell and one derived from the forespore (22,34). Following this in Stage IV, the spore cortex is synthesized, which is a layer of spore-specific PG that resides between the two membranes. The germ cell wall that separates the inner spore membrane from the core is also made during this stage (22,34). Stage V is characterized by spore coat formation, where the mother cell deposits the proteinaceous outer layer on

the spore (22,34). Exosporium synthesis in spore forming *Bacillus* species that contain this layer also occurs in Stage V. Lastly, during Stage VI, spore maturation occurs and the spore acquires the remainder of its resistance properties and in Stage VII the mother cell lyses, releasing the fully developed spore into the environment (22,34). Here, the spore can remain dormant for many years until favorable environmental conditions arise, and the process of germination begins.

1-5 Spore Germination and Outgrowth

The process of spore germination in many respects is the reverse of sporulation. During germination, the dormant spore returns to life, losing its resistance properties, and regaining metabolic activity during outgrowth, after which the spore is converted into an actively growing cell (Figure 1-4). The entire process begins when the spore senses that environmental conditions are once again favorable for vegetative growth, and similar to sporulation, spore germination features many distinct cellular changes. At the onset of germination there is an activation phase of which little is known, but in the laboratory a sublethal heat-shock is generally used to activate *B. subtilis* (48). In nature, the presence of specific nutrients is likely what triggers spore germination, where these nutrients bind in a stereospecific manner to the GRs. In *B. subtilis* spores, L-alanine, L-valine, and L-asparagine trigger germination, and single amino acid changes in a GR subunit can alter the specificity or concentration dependence of the GR's response to a nutrient germinant (2,10,55). However, before germinants can trigger germination, they must first gain access to the GRs, which is likely facilitated through the GerP proteins in the spore coat (4).

After nutrient germinants mix with spores there is a lag period prior to observable events that ranges from a few minutes to >24 hr for individual spores, for unknown reasons, which creates enormous heterogeneity in germinating spore populations. A small fraction of spores show incredibly long lag periods in nutrient germination and are termed superdormant (SD), likely due to very low numbers of GRs in the IM (27,88). Once nutrients presumably bind to the GRs, spores are irreversible bound to germinate, and this step is known as commitment. It is not known precisely what happens in commitment, but it is associated with a change in IM permeability as monovalent cations (H^+, K^+, and Na^+) are released (113), followed by some slow release of CaDPA, and then much faster release of CaDPA (67,88). The release of most CaDPA occurs in only a few minutes for individual spores and all CaDPA release is most likely through channels composed of the seven SpoVA proteins (88,104,105). As CaDPA exits the spore core, water enters, partially hydrating the core and causing loss of heat resistance, however, there is still no metabolic or enzyme activity inside the spore.

CaDPA release completes stage I of germination and triggers the start of stage II, where the CLEs degrade the PG cortex. In *B. subtilis* there are two major redundant CLEs, CwlJ and SleB, which are both likely lytic transglycoylases (96). CwlJ and SleB recognize spore cortex PG due to a specific modification in the peptidoglycan structure, MAL (24,74), which is not present in the germ cell wall or growing vegetative cell PG. CwlJ is activated during germination by CaDPA released from the spore core and can also be activated by exogenous CaDPA. The method of activation for SleB remains unclear. Hydrolysis of the cortical PG allows for the expansion of the spore core, which takes up more water and expands. The IM surface area also increases 1.5- to 2-fold

during this time period, and does so without new membrane synthesis or ATP production (12). At the completion of stage II of germination, the spore core contains roughly 80% wet weight as water and enzymes become active in the core (61). This leads to degradation of the SASP in the spore core and the initiation of metabolism and macromolecular synthesis in the core, and also the partial breakdown of the spore coat. This presumably occurs via proteolysis, and allows for the now metabolically active and outgrowing spore to escape the spore coat and exosporium (if present) (71,91), ultimately becoming a vegetative cell.

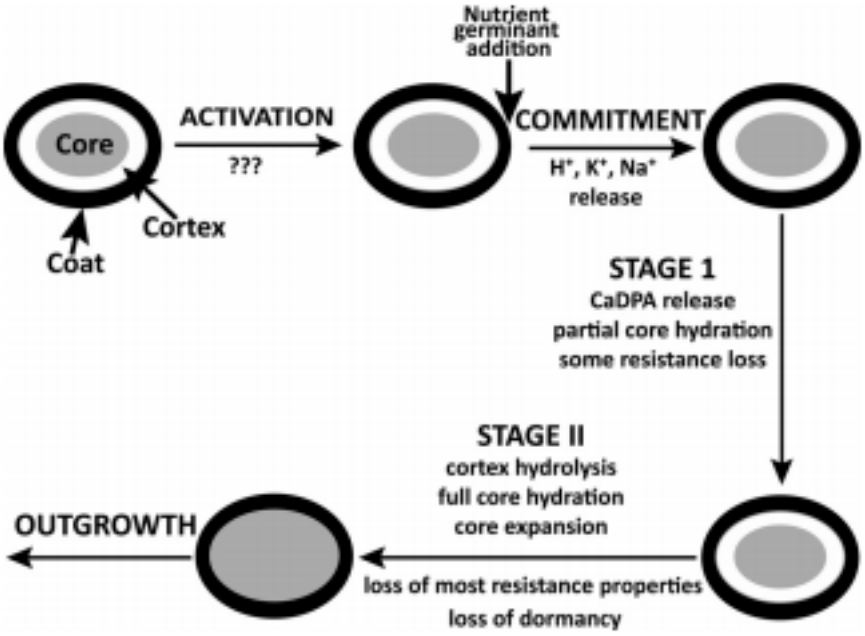

FIGURE 1-4 Outline of nutrient germination of spores of *Bacillus* species (adapted from 88). The steps involved in the activation step are not known and denoted as question marks. Once nutrient addition occurs, the first step in germination is commitment, and the release of monovalent cations is associated with commitment. The germ cell wall is not shown in this figure, but it somehow expands in stage II of germination as the cortex is hydrolyzed, just as the spore core and IM expand ~1.5-2-fold.

1-6 Germinant Receptors (GRs)

Germination of *B. subtilis* spores normally begins with binding of specific nutrient germinants, either L-alanine or a mixture of L-asparagine, D-glucose, D-fructose, and potassium ions (AGFK), to their cognate germinant receptors (GRs) located in the IM (30,59,84,88). In *B. subtilis*, there are three functional GRs, each encoded by homologous tricistronic, *gerA, gerB,* and *gerK* operons. The GerA GR responds to L-valine, the GerB and GerK GRs cooperate to respond to AGFK (84). When all three GRs are deleted, spores fail to germinate with nutrients but a slow spontaneous rate of germination occurs, which is still not understood (58).

Bioinformatics analysis indicates that the A subunit of GRs likely has 4-6 transmembrane (TM) segments plus a large N-terminal hydrophilic domain and a small hydrophilic C-terminal segment. (42,111). The B subunit of GRs are predicted to be hydrophobic, with 10-12 TM domains. Much like the GerD protein (see below), the C subunit of GRs are IM lipoproteins, which are situated on the outer face of the spore IM (42, 111). The structure of most of the *B. subtilis* GR's C subunit has been determined by X-ray crystallography (46), but has not yielded any specific insight into C subunit function.

The levels of GRs in individual spores vary significantly depending on sporulation conditions; rich medium leads to higher GR levels than with poor media (35,81). When sporulated in rich medium, levels of individual GRs in *B. subtilis* range from 600-1100 molecules per spore (94), and in poor medium thes level of GR can be 3- to 8-fold lower. The regulation of GR subunit genes is complex in *B. subtilis*, with

regulation by medium composition occurring in some unknown way, and also by at least two auxiliary transcription factors, SpoVT and YlyA, which control levels of GR subunits in individual sporulating cells (75,102). As a result of this complex regulation, GR levels appear to vary significantly between spore populations made differently, as well as between individual spores in a population, with stochastic effects on regulatory protein levels and GR expression levels also contributing to the wide variation of GR levels seen in individuals in spore populations (30,87,103).

1-7 Non-Nutrient Germination

There are alternative pathways in which *B. subtilis* spores germinate that do not involve the GRs. A detailed overview of both nutrient and non-nutrient germination is outlined in Figure 1-5. Specific agents that trigger non-nutrient germination are CaDPA, cationic surfactants, in particular dodecylamine, hydrostatic pressure (HP), PG fragments, and lysozyme or other PG hydrolases (86). Lysozyme is known to degrade the spore cortex in spores whose coats are permeabilized, but it also degrades the germ cell wall, allowing the spores to lyse. However, if germination is induced in a hypertonic medium, spores retain their structure, the PG cortex is degraded, and DPA is released allowing the spores to germinate and outgrow (74,84). CaDPA has been suggested to function in germination by direct or indirect activation of CwlJ, although the exact mechanism of activation is unknown (60). However, cationic surfactants like dodecylamine have been shown to open the spore's CaDPA channels (84,103), in which the SpoVAC protein likely acts as a mechanosensitive channel, operation of which does not require GRs (104).

The non-nutrient germinant that has significant applied importance is HP pressures of 1000s of atmospheres. Generally, HP of 50-350 megaPascals (MPa) trigger spore germination via activation of the spores' GRs, while higher pressures trigger germination via direct activation of CaDPA release from the spores, likely through activation of a CaDPA channel composed of the SpoVA proteins (40,86). Pressures greater than 500 MPa and elevated temperatures are used in food processing applications to pasteurize and sterilize products with long shelf lives (87).

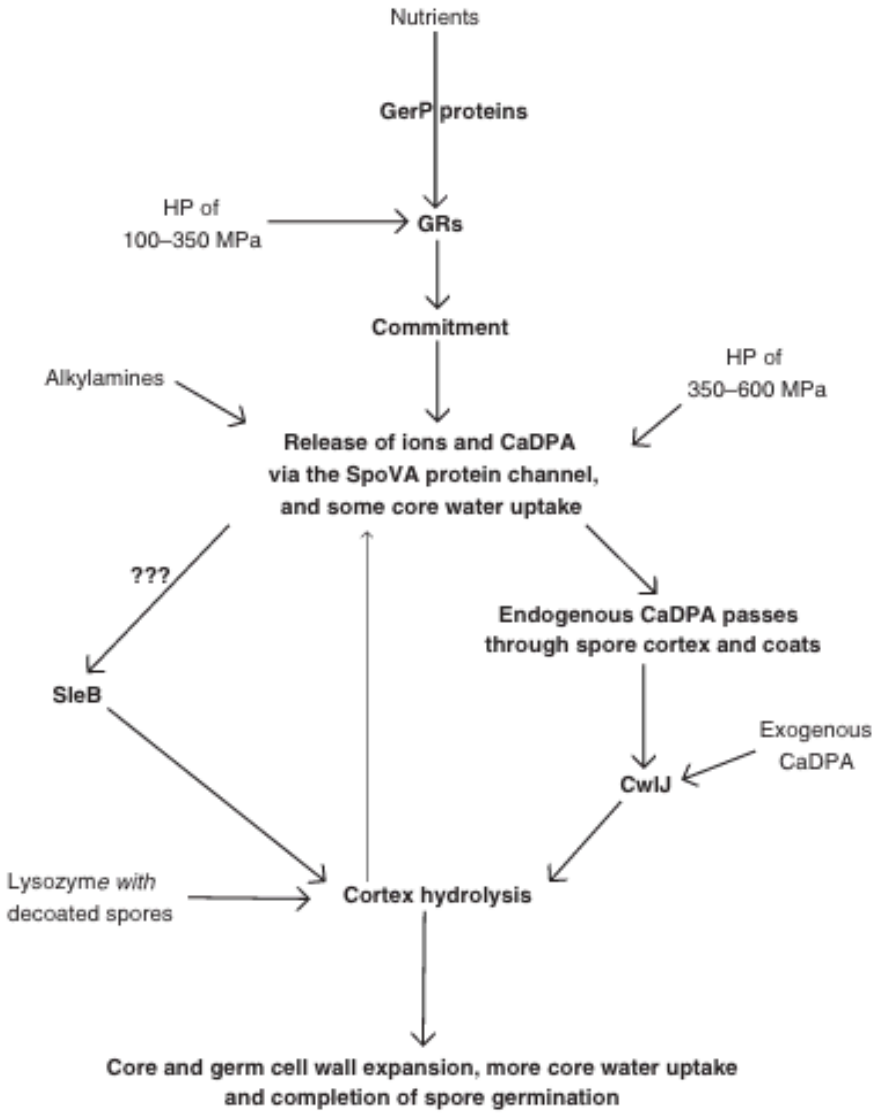

FIGURE 1-5 Overview of nutrient and non-nutrient germination in a *Bacillus* spore (adapted from 87). Nutrients access the GRs via the GerP proteins, but the exact method of access is unknown. It is likely that alkyamines like dodecylamine and HP of 350-600 MPa directly open an SpoVA channel, although this has not been proven definitively. The mechanism for SleB activation remains unknown. There is also some mechanism(s) by which cortex hydrolysis occurs via lysozyme, triggering ion and CaDPA release.

1-8 Accessory Germination Protein - GerD

Another protein known to be involved in *B. subtilis* germination is GerD, a ~20 kDa, 180 residue lipoprotein with a putative 11 amino acid signal sequence and a putative recognition sequence for diacylglycerol addition to a specific cysteine residue near the protein's N-terminus (47,99). GerD is located on the outer surface of the spore IM, where it most likely exists as a peripheral IM protein held by a diacylglycerol anchor (37,82). Spores of *B. subtilis* mutants lacking GerD exhibit decreased rates of germination with al GR-dependent germinants, but germinate normally with GR-independent germinants (65), consistent with GerD acting as a mediator of signal transduction in nutrient germination. Given that in *Bacillus* spores, both the SpoVA proteins and the germination-specific CLE SleB are also located in the spore IM (64,105,106), it is possible that GerD plays a role in mediating the rapid transduction of signals from the GRs to downstream effectors.

Synthesis of *gerD* in the developing forespore is under the control of RNA-polymerase sigma factor σ^G, as are the *gerA, gerB, gerK,* and *spoVA* operons (33,107), which are made ~3 h prior to forespores' CaDPA accumulation (61,84). The crystal structure of 2/3rd of the *Geobacillus stearothermophilus* GerD was solved at 2.7-Å resolution, and shows the protein forms a stable α-helical trimer that can superimpose upon itself to form higher order structures (Fig. 1-6) (47). Furthermore, the GRs and GerD have been shown to colocalize in dormant spores' IM and up through stage I of germination in a discrete cluster termed "the germinosome," which is dependent upon GerD to form in dormant spores (30,103). The sequence of GerD is well conserved among bacilli, but GerD is not preset in spores of clostridia (62,111). Furthermore, the

GerD protein does not resemble any GR protein, nor does it share homology with any known proteins.

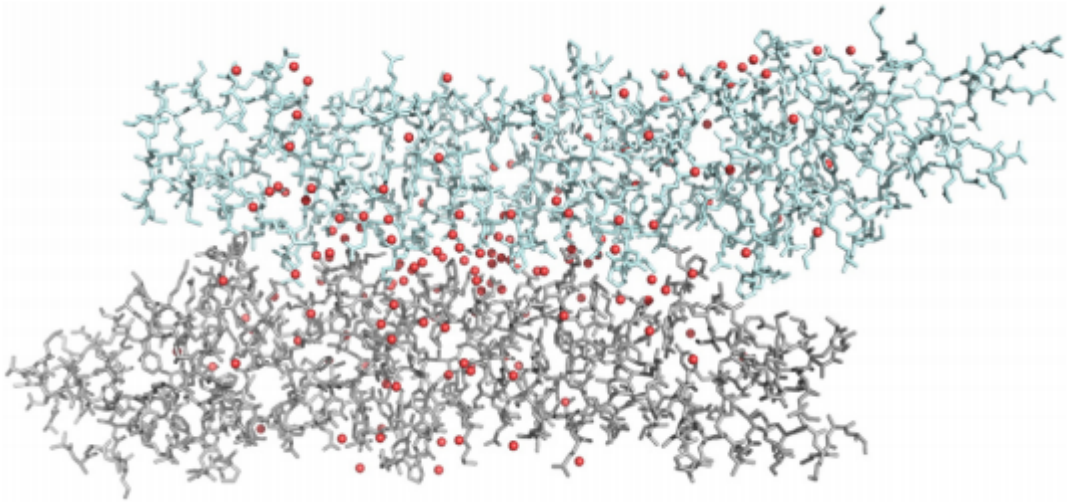

FIGURE 1-6 Side view of two GerD$^{60\text{-}180}$ trimers in the asymmetry unit (47). When superimposed on each other asymmetrically a distinctive packing arrangement can be seen laterally along the crystal structure of GerD's superhelical axes. The crystal structure of the 121-residue core domain from *Geobacillus stearothermophilus* GerD was solved at a resolution of 2.7-Å. The crystal structure revealed that GerD exists as a trimer with three parallel helical polypeptide chains wrapping into a supercoiled rope. Water molecules are depicted as red spheres.

1-9 The Germinosome

The formation of the cluster of germination proteins in the IM, termed the germinosome, involves the GerA, GerB, and GerK GRs and GerD, and forms in a GerD-dependent manner (30,103). In dormant spores, GerD forms a single IM cluster even in the absence of the GRs, however upon deleting *gerD*, the GRs fail to colocalize and instead are diffusely distributed throughout the IM (30,103). Moreover, the loss of GerD also causes a significant decrease in spore germination rates with nutrient germinants, which further supports the significance of the germinosome and GerD in spore germination. However, the mechanism for GerD mediated effects on spore germination remains unknown (65).

It was recently found that after initiating spore germination, the germinosome foci ultimately change into larger disperse patterns, with ≥ 75% of spore populations displaying this pattern in spores germinated for one h, although >80% of spores germinated for 30 min retained the germinosome foci (103). Furthermore, levels of GerD dropped ~ 50% within 15 min in germinated spores (103). Therefore, because this drop in GerD occurred faster than the dispersion of the germinosome, it is likely that germinosome stability in germination is determined by other factors, such as restoration of rapid IM lipid mobility or the expansion of the IM ~2 fold.

The germinosome also forms in sporulation nearly in parallel with GR and GerD synthesis soon after engulfment of the developing spore occurs (Troiano, unpublished), ~3 h before DPA accumulation, and before spore maturation when the IM condenses and IM lipids become immobile. Again, even in strains that lacked all the GRs, GerD was found to self-associate into discrete foci, indicating the protein self-associates in

sporulation. Many questions still remain about the germinosome, in particular concerning the interactions that hold proteins together in this complex. While GerD has been shown to colocalize to itself (30), the same does not hold true for any of the GRs, as they require all three subunits and GerD to properly assemble into the germinosome.

1-10 Specific Aims

In *Bacillus subtilis*, the mechanisms of spore germination have been extensively studied, but much remains unknown. Currently, the process of signal transduction in spore germination is poorly understood, as how signals from the environment go from activating GRs to downstream effectors, ultimately leading to CaDPA release are not known. It is now known that the GRs and an accessory lipoprotein, GerD, colocalize in dormant spores in a GerD dependent manner, creating a spore germination protein complex known as the "germinosome." The functional role of this novel protein complex in *B. subtilis* spore germination is not understood. As a result, we propose to examine the dynamics of the germinosome in *B. subtilis* spores by studying its dynamics in spore germination, as well as its formation in sporulation, in order to better understand its function as well as the organization of its constituents. We hypothesize that germinosome formation, localization, and function is dependent upon GerD and protein-protein interactions within the complex. By better understanding this protein receptor complex, perhaps we will gain some further knowledge about germination signal transduction.

A. Examining the formation of the germinosome

It is known that GRs and GerD are synthesized under the control of the same RNA polymerase sigma factor, σ^G during late stage sporulation (107). In addition, the genes encoding SASP are also under the control of σ^G and expressed at much higher levels than the GRs (83,107). While it is known that σ^G becomes active after forespore engulfment in sporulation (96,107), by utilizing *lacZ-ssp* fusions, we can more accurately pinpoint when the germination proteins are synthesized during sporulation. As a result, we can use this timeframe information to analyze the fluorescent foci localization patterns of the GRs and GerD. To do this we will use fluorescent fusions to GR and GerD proteins, plus epifluorescence microscopy to examine the formation of the germinosome in sporulating *B. subtilis* cells.

Using a Δ*gerD* background, we can test the dependence of the germinosome's formation on GerD. We expect the germinosome forms in a GerD dependent manner, but perhaps not immediately after GR/GerD synthesis, due in part to lipid mobility of the IM at that time in sporulation. As the developing spore matures, lipids within the inner spore membrane become largely immobile and the membrane compresses (12), although it is not known precisely when this happens in sporulation. This IM compression could force germinosome proteins into close proximity and allow for protein-protein interactions. We believe that GerD acts as staging platform for the germinosome, self-associating in the spore IM and facilitating the formation of the germinosome in concert with the compression of the inner membrane. Understanding the formation of the germinosome may be critical in understanding its role in signal transduction, and how it functions in germination.

B. Analyzing germinosome dynamics in spore germination and outgrowth

It is known that the germinosome exists in dormant spores in a GerD dependent manner and abolishing germination protein clustering correlates with loss or significant reduction in the ability of spores to germinate (30), but it is still not known why. No knowledge exists concerning the germinosome and its behavior in germination, but it is known that GerD protein levels diminish in germinated spores (66). Therefore, we hypothesize that as GerD levels decrease in germinating spore populations, the germinosome proteins will dissipate consistent with the idea that colocalization of GRs is dependent on GerD. To test this, we propose to use the same fluorescent protein fusions in aim (A) to study the germinosome and its constituent proteins during germination and outgrowth through time-lapse epifluorescence microscopy. In addition we will use Western blotting to detect protein levels during germination and outgrowth.

In addition, because the process of germination has many specific and important events, we propose to use fluorescent germination protein fusions in a Δ*cwlD* background, in which cortex PG does not contain MAL and is not degraded by CLEs. Individual spores with this mutation are unable to progress beyond stage I of germination, and as a result, the core does not expand, the IM does not expand, and IM lipid mobility is not restored. By utilizing a *cwlD* mutant strain, we can better understand how the germinosome behaves in the different stages of germination. Understanding the dynamics of the germinosome and GerD in the context of germination will be critical in our understanding of germination as a whole, and perhaps may yield some clues as to how the complex facilitates signal transduction to downstream effectors.

CHAPTER 2

GERMINOSOME FORMATION IN SPORULATION

Analysis of the formation of a spore germination protein complex during *Bacillus subtilis* sporulation

Anthony J. Troiano Jr.[1], Ann E. Cowan[1], Ji Yu[2], Qingfen Yang[2] and Peter Setlow[1]*

Departments of [1]Molecular Biology and Biophysics, and [2]Cell Biology

UConn Health

Farmington, CT 06030

Running title: Formation of the germinosome during sporulation

Key words: *Bacillus*, spores, sporulation, germinant receptors, GerD, germinosome

*Corresponding author

Address: Department of Molecular Biology and Biophysics, UConn Health, Farmington, CT 06030-3305

Phone: 860-679-2607

Fax: 860-679-2308

Email: setlow@nso2.uchc.edu

CHAPTER 2 – CONTRIBUTIONS

The majority of work completed in chapter two was performed by Anthony J. Troiano Jr. in Peter Setlow's laboratory, which includes spore preparation of all *Bacillus subtilis* strains, biochemical analyses of b-galactosidase activity, and DPA assays. Microscopy analysis of sporulating bacteria was perfomed by Anthony J. Troiano Jr. on Ji Yu's custom epifluorescence Nikon microscope, and subsequent data analysis of germinosome quantitation was done by Anthony J. Troiano Jr. Fluorescence image analysis and guassian distribution curve fitting was performed by Anthony J. Troiano Jr. under the supervision of Ann E. Cowan, as well as all photoshop and ImageJ work. All luorescent fusion strains of *B. subtilis* used were created previously in the lab by Keren Griffiths.

Creation of *E. coli* strains was performed by Qingfen Yang in Ji Yu's laboratory. Microscopic analysis of fluorescent labled *E. coli* was done by Ji Yu, as well as subsesquent data analysis, and is credited for writing all information regarding *E. coli* strain construction and microscopy in the methods of this chapter as well as Figure 2-5.

2-1 ABSTRACT

When faced with nutrient starvation *Bacillus subtilis*, a Gram-positive soil microbe, initiates the process of sporulation, forming a morphologically distinct and metabolically dormant spore. However, when nutrient signals from the environment interact with germinant receptors (GRs) in the spores' inner membrane (IM), an environment in which the lipids are immobile, spores normally undergo the process of germination, ultimately turning back into a growing cell. GRs and another accessory germination protein, GerD, have been shown to colocalize in dormant spores' IM, and remain colocalized early in spore germination in a complex termed the "germinosome." To understand how the germinosome forms in sporulation, differential interference contrast and epifluorescence microscopy were used to monitor locations of different fluorescent reporters fused to germination proteins throughout sporulation. This work found that the germinosome forms almost in parallel with GR and GerD synthesis soon after mother cell engulfment of the forespore spore in sporulation, ~3 h before dipicolinic acid accumulation. In strains that lacked all GRs and had a single *gerD-gfp* fusion, discrete fluorescent foci were still observed, indicating that GerD can self-associate in sporulation. When GerD-GFPmut1s was expressed in growing *B. subtilis* cells, the protein also self-associated as did GerD-Venus in growing *Escherichia coli*. In addition, when a GR-mCherry fusion was expressed in *E. coli*, no distinct foci were seen until GerD was also expressed. Together, these results are consistent with GerD acting as a scaffold for germinosome formation.

2-2 INTRODUCTION

Some bacteria respond to nutrient starvation by forming an endospore, a morphologically distinct cell type, in a process known as sporulation (33). Spores of *Bacillus* and *Clostridium* species are metabolically dormant and resistant to harsh environmental stresses, allowing them to survive for many years (85). Once specific nutrients are present, the process of germination is triggered and spores lose their dormancy and resistance, outgrowing back into a vegetative cell. In order for germination to occur, nutrients must traverse the dormant spore coat, outer membrane, cortex, and germ cell wall to reach the nutrient germinant receptors (GRs) located in the spore inner membrane (IM) (88). In the *B. subtilis* spore IM, lipid molecules are largely immobile, but upon completion of spore germination, the IM surface area expands 1.5 to 2-fold and lipid mobility increases significantly, all in the absence of detectable ATP synthesis (12). Once specific nutrients bind to their cognate GRs, the spore core releases its large depot (~25% of core dry wt) of dipicolinic acid (DPA) chelated to divalent cations, mostly Ca^{2+} (CaDPA). The release of CaDPA also triggers degradation of the spore's peptidoglycan (PG) cortex by cortex-lytic enzymes (CLEs), permitting core expansion, additional core water uptake, completion of germination, and ultimately outgrowth into a vegetative cell (88).

In *B. subtilis* spores, three functional GRs have been identified, GerA, GerB, and GerK, each encoded by a homologous tricistronic operon producing two polytopic integral transmembrane proteins (A and B subunits) and a peripheral membrane lipoprotein (C subunit). The GRs, as well as GerD, a lipoprotein essential for rapid GR-dependent germination, have been shown to colocalize in a small focus in dormant *B.*

subtilis spores IMs in a structure termed the germinosome (30). If *gerD* is deleted, the GRs fail to colocalize and instead are diffusely distributed throughout the IM, suggesting that GerD facilitates germinosome formation; indeed, GerD itself localizes in a small focus in dormant spores' IM in the absence of all GRs. Other germination proteins, such as the 7 SpoVA proteins, most of which are integral membrane proteins involved in CaDPA movement into and out of the spore in sporulation and germination, are not associated with the germinosome in dormant spores, nor do they seem to affect its fate in spore germination (30,45,68,103,106).

A recent study has shown that in germinating spores the germinosome foci ultimately disperse into larger diffuse patterns, with ≥ 75% of spore populations displaying this pattern in spores germinated for one h (103). However, > 80% of spores germinated for 30 min retain germinosome foci, while levels of GerD decrease ~50% within 15 min in germinated spores. Spore cortex PG has high levels of the cortex-specific modification muramic acid-δ-lactam, which is a recognition determinant for cortex-lytic enzymes that degrade cortex PG in stage II of germination (88). The CwlD protein is essential for formation of muramic acid-δ-lactam in cortex PG, and consequently, *cwlD* spores cannot progress beyond stage I of germination and germinosome dispersion does not occur (74,103). Therefore, in germinating spores, factors other than GerD levels, such as core expansion and restoration of rapid IM lipid mobility, could be important in determining the fate of the germinosome following spore germination. Given the apparent crucial role of the germinosome in rapid spore germination, understanding the dynamics of germinosome assembly and disassembly will

be critical to the understanding the mechanisms of and signal transduction in spore germination (88,103).

While the fate of the germinosome during spore germination and outgrowth, as well as factors important in germinosome formation in spores, have been studied (30,103), the mechanism by which the germinosome forms in sporulation is unknown. It is known that synthesis of GRs and GerD take place in parallel during sporulation under the control of the same RNA polymerase transcription factor in sporulation, σ^G, a forespore specific sigma factor that is activated once engulfment of the developing endospore is complete (97,98,107). In addition, GerD and GerF, a diacylglycerol transferase involved in lipid addition to GR C-subunits and GerD, are essential for both germinosome formation in dormant spores, as well as rapid nutrient germination (30,37). Although normal GerD levels are not essential for maintaining germinosome stability in germinating spores, it is possible that GerD is required for germinosome formation in sporulation, and that because the genes encoding GRs and GerD are under the control of the same RNA polymerase transcription factor, this complex forms in parallel with GerD and GR synthesis. This would suggest that during sporulation the germinosome might form before compression of the spore IM and immobilization of IM lipids, and the germinosome constituents do not form foci simply because they are forced into close proximity with one another late in sporulation. Understanding the formation of the germinosome in *B. subtilis* sporulation might lead to clues about mechanisms of signal transduction in spore germination. Consequently, in this work we have examined the kinetics of germinosome formation during *B. subtilis* sporulation, and have compared the kinetics to other events taking place in developing forespores.

2-3 MATERIALS AND METHODS

***B. subtilis* strains and spore preparation.** *B. subtilis* strains used in this work are listed in Table 2-1 and are isogenic with strain PS832, a prototrophic 168 laboratory strain. The fluorescent fusion strains are all isogenic derivatives of PS4150, derived from PS832 and missing two genes essential for spore coat assembly, *cotE* and *gerE* (28). Loss of these two genes results in greatly reduced autofluorescence in the coatless PS4150 spores, allowing visualization of fluorescence from GFP derivatives fused to germination proteins. The fusion strains are: i) KGB73 with a *gfp* sequence fused to the C-terminal coding end of the *gerD* gene at the *gerD* locus and that retains an expressed wild-type *gerD* gene; ii) KGB80 with a *gerKB-mCherry* fusion from strain KGB72 and the *gerD-gfp* fusion from strain KGB73; iii) KGB114 with a *gerAA-mCherry* sequence inserted at the *amyE* locus downstream of the native promoter for the *gerA* operon encoding the GerA GR; iv) KGB123 which is strain KGB73 transformed to Cm^r using chromosomal DNA from strain PS3476 (*sspA-lacZ*) that carries a *lacZ* fusion to the *sspA* gene encoding a small, acid-soluble protein important for protecting spore DNA from chemical and enzymatic cleavage (85), SspA is synthesized in developing spores in parallel with GRs and GerD (12-14); v) KGB196 which is strain KGB114 transformed to Km^r with plasmid pPS2379 (pCm::Km) (30) and with KGB171 (Δ*gerD*::Cm) (gift of Keren Griffiths) chromosomal DNA that carries a deletion of the *gerD* gene essential for germinosome formation and nutrient germination (30,47,88); and vi) KGB213 which is KGB164 (*gerD-gfp*) transformed to Km^r and MLS^r using chromosomal PS3609 DNA carrying a deletion of the *gerA* operon (37), chromosomal FB41 DNA carrying a deletion of the *gerB* operon (56), and chromosomal PS3418 carrying a deletion of the *gerK* operon (37).

All strains created for imaging of live cells were done so by Dr. Ji Yu's laboratory and are described in this section. *E. coli* strains used in this work are listed in Table 2-2. GerD and GerAC sequences from *Bacillus subtilis* were cloned into *E. coli* expression plasmids, giving expression of GerD-Venus alone, GerAC-mCherry alone, or both GerAC-mCherry and GerD. The GerD-Venus fusion was used instead of GerD-GFP as the Venus fluorophore produced the best signal to noise ratio in *E. coli*. To generate the GerD-Venus expression clone (pQY4), a gateway cloning strategy was used. Namely, the *gerD* gene sequence (without the stop codon) was amplified by PCR and subcloned into an entry vector (pENTR/SD/D-TOPO, ThermoFisher, Waltham, MA) to form the entry clone pENTR-GerD. The entry clone was then used to react with a gateway vector carrying the p*Lac-attR-venus* sequence (*attR* is the gateway recombination cassette) using gateway LR clonase (ThermoFisher), which catalyzes recombination between the entry clone and the gateway vector. The result is the transfer of *gerD* sequence to replace the *attR* gateway recombination cassette, producing the *gerD-venus* fusion under the control of the promoter for the *E. coli lac* operon. The resultant plasmid was used to transform *E. coli* K12 cells, and the transformed strain was used for imaging. The plasmid for GerAC-mCherry expression (pQY96) was generated in a similar manner, by recombining a *gerAC* entry clone plasmid with a gateway vector carrying the p*BAD-attR-mCherry* sequence giving an *E. coli* K12 strain with *gerAC-mCherry* under the control of the arabinose promoter. Finally, for co-expression of GerAC-mCherry and GerD, an intact *gerD* gene was cloned in the PmeI site following the *gerAC-mcherry* sequence in plasmid pQY96, giving plasmid pJQ61.3 in *E. coli* K12.

Biochemical analyses. For assays of β-galactosidase activity, the optical density at OD_{600} of sporulating KGB123 spore cultures was determined every h, 1 mL samples centrifuged at 13,000 x *g* and pellets were suspended in 1 mL 25 mM Tris-HCl buffer (pH 7.4). Pellets were centrifuged again at 13,000 x *g* and resuspended in 0.5 mL Z buffer (0.06 M $Na_2HPO_4 \cdot 7H_2O$, 0.04 M $NaH_2PO_4 \cdot H_2O$, 0.01 M KCl, 0.001 M $MgSO_4$, 0.05 M β-mercaptoethanol [pH 7.4]). Samples in Z-buffer were incubated for 15 min at 37°C, 10 μL 10% Triton X-100 added, and the mixture was vortexed for 30 sec, and kept on ice. 300-400 μL of lysed cells were transferred to a new microcentrifuge tube and made to 800 μL with Z-buffer. Samples were pre-incubated for 2 min at 30°C, 160 μL ortho-nitrophenyl-β-galactoside (4 mg/mL) substrate added, the mixture incubated at 30°C until visibly yellow, the reaction stopped by addition of 0.4 mL 1 M Na_2CO_3, and the mixture vortexed and kept on ice. After reactions were stopped, the samples were centrifuged for 10 min at 13,000 x *g* and 1 mL of supernatant fluid was pipetted to new tubes. The OD_{420} of the supernatant fluids was read in a spectrophotometer, and β-galactosidase specific activity was calculated as Miller units using the formula $(OD_{420})(1000)/(\text{volume of culture assayed in mL})(\text{reaction time in min})(OD_{600})$. β-galactosidase specific activity was then graphed as a percentage of the maximum Miller units observed.

For DPA assays, 1 mL of sporulating *B. subtilis* cultures at various time-points were centrifuged at 13,000 x *g* for 5 min, pellets washed in 1 ml phosphate buffered saline (PBS) (50 mM NaH_2PO_4, 150 mM NaCl [pH 7.2]) and centrifuged again before being suspended in 1 ml H_2O, and boiled for 30 min. After boiling, samples were put on ice for 15 min, and then centrifuged at 15,000 x *g* for 15 min. Supernatant fluids were

transferred to new microcentrifuge tubes, and 50 μl supernatant fluid, 50 μl 100 mM K-Hepes buffer (pH 7.4) with 200 μM $TbCl_3$ and 100 μL of H_2O was added to wells in a 96-well plate for a fluorescence plate reader. Tb-DPA fluorescence was measured using a SpectraMax fluorescence plate reader (Molecular Devices, Sunnyvale, CA) using excitation at 270 nm and emission at 545 nm. DPA levels were graphed as a percentage of the maximum level observed.

Microscopy. For fluorescence microscopy, sporulating cultures were grown as described above, and 1 mL samples were taken at 30 min time-points from 10-20 h after culture inoculation. Samples were immediately centrifuged at 13,000 x *g*, the pellet suspended in 50 μL PBS, and 2 μL of the suspension was pipetted between two sterile glass cover slips. Epifluorescence and differential interference microscopy (DIC) images were taken of the sporulating cultures as described previously (30,102), and images were processed using ImageJ and Adobe Photoshop software. For publication, enlarged images were scaled to 300 pixels/inch using a bicubic function. Due to the poor signal to noise ratio in the spores and inherent autofluorescence from sporulating cells, we acquired 50-70 consecutive images at each time point with an acquisition time of ~75 ms. Increasing the number of images taken or increasing the acquisition time resulted in significant photobleaching. Images used in subsequent analysis were generated as described previously (30,103). In determining co-localization of the signal from double fluorescent protein fusion strains, if the maximum intensities of the two signals were ≤ 1 pixel apart, they were scored as colocalized, as the positions of the mCherry and GFP foci can be partially shifted due to signal noise and the wavefront alteration caused by changing of the dichroic mirrors. Fluorescence distribution curves along the long axis of released

spores and spores still contained within mother cells were generated as described previously. Plots of σ, or the width of the Gaussian distribution at (1/e) the maximum fluorescence intensity, were generated, and P-values calculated from the student's two-tailed t-test.

For imaging studies with *E. coli*, cells of strains with GerD or GerAC-fusions or both were grown overnight at 37°C in LB medium. The latter culture was diluted 1:100 in M9 medium ((g/L): $Na_2HPO_4 \bullet 2H_2O$ (4.5), KH_2PO_4 (3), NaCl (0.5), NH_4Cl (1), $CaCl_2$ (0.011), $MgSO_4$ (0.24), glucose (2)) and supplemented with either 0.1 mM IPTG or 0.2% arabinose to induce gene expression from the lactose or arabinose promoters, respectively. After 2 h of growth at 37°C, cells were harvested, concentrated and imaged as described above for growing *B. subtilis* cells.

2-4 RESULTS

Germinosome foci in developing endospores and released spores with single fluorescent fusions are identical. To study the germinosome during *B. subtilis* sporulation, we first used strains with single fluorescent fusions to germination proteins to determine whether the signal to noise ratio in our system would be sufficient to allow for effective epifluorescence microscopy. Specifically, we examined strain KGB114 (PS4150 *gerAA-mCherry*) using DIC and epifluorescence microscopy, and analyzed sporulating cells at 30 min time intervals between 10-14 h in culture. Unlike mature released spores, developing spores are still contained within the mother cell compartment of the sporulating cell, as can readily be seen in the DIC channel (Fig. 2-1A). However, both released and mother cell-retained spores show nearly identical fluorescent germinosome foci (Fig. 2-1B-C).

In order to compare spore fluorescence quantitatively, the fluorescence intensity of 20 spores still in the sporangium and 20 released spores were measured along their long axes. The full width at half maximal intensity for released KGB114 dormant spores was ~300 nm (data not shown), as seen previously (30,102), indicative of the maximum germinosome size and resolution limit of the microscope. The fluorescence intensity distributions were fit to Gaussian distributions and and these curves were averaged (Fig. 2-1D; black and light grey curves); similar average Gaussian fits were determined for sporulating KGB196 (PS4150, Δ*gerD gerAA-mCherry*), which cannot form a germinosome due to lack of GerD (Fig. 2-1D: dark grey curve). The average Gaussian distribution for KGB114 spores in sporangia and mature released spores were similar to those seen previously for dormant spores with comparable fluorescent fusions (30,103).

However, there is a significant difference in the distribution of the fluorescence signal between KGB114 and KGB196 spores (Fig. 2-1D). To further compare this difference, we determined σ, or the width of the Gaussian distribution curve at (1/e) of the maximum fluorescence intensity, in all three spore populations (Fig. 2-1E). There was no difference in σ between KGB114 spores in sporangia and released spores; however, there was a statistically significant increase in σ determined for KGB196 *gerD* spores compared to KGB114 and(Fig. 2-1E). This difference shows that fluorescence in KGB114 spores in sporangia and released spores is localized to discrete foci that we have termed germinosomes. To better understand when the germinosome first appears, we quantified the percentages of cells with fluorescent foci in sporulating cell populations (Fig. 2-1F). Fluorescence signals were first detected at h 11 of culture (~20% foci) and reached ~80% foci by h 12 (Fig. 2-1F). Thus, in sporulating KGB114 populations, germinosome foci appeared immediately after the fluorescence signal became detectable.

Germinosome foci in sporulating double fluorescent fusion strains colocalize. To further understand how the germinosome forms in sporulation, sporulating KGB80 (PS4150 *gerKB-mCherry gerD-gfp*) populations were also examined using DIC and fluorescence microscopy. Images were acquired after 12.5 h of culture (Fig. 2-2Ai-iv), and both GerKB-mCherry and GerD-GFP fluorescent foci appeared colocalized in discrete foci in both developing spores in sporangia and released spores (Fig. 2-2Aiv). To further quantitate germinosome formation in this double fusion strain, the total fluorescence intensity along the long axis of multiple individual spores in sporangia and released spores with colocalized foci were measured across sporulating populations, and the data were fit to a Gaussian distribution and averaged (Fig. 2-2B). The latter analysis

allowed determination of values for σ for KGB80 spores in sporangia and released spores, which were plotted along with data from spores in sporangia of KGB196 (PS4150, Δ*gerD gerAA-mCherry*) as a negative control (Fig. 2-2B,C). As was the case with single fluorescent fusions, there was no difference in σ values between developing spores in sporangia and released mature spores in the double fluorescent fusion strain, but there was a noticeable difference between KGB80 and KGB196 *gerD* null spores, and this change was statistically significant.

To better understand the timing of the appearance of germinosome foci in sporulation, the per cent of cells with foci (Fig. 2-2C, black line) and DPA (Fig. 2-2C, grey line) were plotted as a percentage of maximum levels observed during time in culture. It is important to note that the maximum percentage of developing sporangia that contained germinosome foci in sporulating cell populations was ~85%, as seen previously for mature spores (30,103). Notably, the maximum percentage of fluorescent foci observed appeared ~ 3 h before the maximum percentage of DPA was accumulated (Fig 2-2D), indicating that the germinosome appears well before DPA accumulation occurs in sporulation. These data also suggest that the germinosome appears in parallel with GerD/GR accumulation, which has been seen previously to be ~ 3 h prior to DPA accumulation under the sporulation conditions used in the current work (52,87).

Germinosome foci appear in parallel with synthesis of GerD and GRs. While the data noted above strongly suggested that germinosome formation paralleled accumulation of GerD and GRs, it was important to demonstrate this point directly. To do this, we first analyzed sporulating KGB123 (PS4150 *gerD-gfp sspA-lacZ*) cells by DIC and fluorescence microscopy (Fig. 2-3A,B) between 10.5-14 h in culture. As noted above

with sporulating cells that contained only *gerD-gfp*, as soon as the GerD-GFP fluorescence signal became detectable in developing spores in sporangia at 11.5 h, discrete foci were seen (Fig. 2-3Aii) indicating germinosome formation. This fluorescence pattern did not change as the spores matured in sporangia and were released from their mother cells at ~ 13.5 h (Fig. 2-3Bii).

In addition to *gerD-gfp*, strain KGB123 also has a *lacZ* translational fusion to the *sspA* gene, encoding a small, acid-soluble protein important for protecting spore DNA (85,86). Importantly, *sspA* expression is under the control of the same RNA polymerase transcription factor (σ^G) that directs *gerD* and GR gene expression, all of which are expressed in parallel in the developing forespore during sporulation (52,93,106). In addition, *sspA-lacZ* is expressed at high levels, making its measurement easy by assay of β-galactosidase (52). To determine when *sspA-lacZ* was expressed relative to germinosome formation, samples of the sporulating KGB123 culture used to analyze germinosome formation were also taken every 30 min from 10.5-19 h, and β-galactosidase specific activity (Fig. 2-3B, dark grey line), and accumulation of DPA and germinosome foci (Fig. 2-3B, grey and black lines, respectively), were determined and calculated as the percentage of the maximum level observed. Again, the maximum percentage of germinosome foci seen was 80-85%, as seen previously (30,102). This experiment showed that the percentage of germinosome foci observed was 80-85% at 13 h, ~3 h before the peak of DPA accumulation at 16 h, and only 30 min before the peak of β-galactosidase specific activity at ~ 13.5 h. The drop in β-galactosidase specific activity after 13.5 h is due to spore maturation, as when spores mature, β-galactosidase in the spore core becomes refractory to lysozyme extraction unless spores are first decoated

(52). This experiment was repeated three times, all with very similar results (data not shown). These data suggest that germinosome foci accumulate largely in parallel with GerD and GR synthesis.

To additionally quantitate germinosome dynamics in sporulating KGB123 cells, the total fluorescence intensity was measured along the long axis of multiple individual endospores and released spores, and the data were fit to a Gaussian distribution and averaged (Fig. 2-3D). The total fluorescence intensity of KGB196 spores fit to a Gaussian distribution was used as a negative control (Fig. 2-3D, dark grey curve). Values for σ were generated from Gaussian distributions and plotted for three data sets (Fig. 2-3E). As was the case for single and double fluorescent fusion strains, no difference was seen between spores in sporangia and released spores, but a significantly higher value of σ was found in Δ*gerD* spores.

GerD forms foci in sporulating cells in the absence of GRs. It is known that GerD-GFP localizes primarily in a single focus in the IM of *B. subtilis* spores even in the absence of all GRs (30,103). To test if GerD-GFP forms foci in sporulating cells lacking GRs with the same kinetics as with KGB123 cells, we sporulated strain KGB213 (PS4150 *gerD-gfp* Δ*gerA* Δ*gerB* Δ*gerK*), which has a *gerD-gfp* fusion but lacks genes for all functional GRs, and analyzed the sporulating cells by DIC and fluorescence microscopy (Fig. 2-4A). Even in developing spores in sporangia that lack all GRs, *gerD-gfp* foci can be seen at ~ h 12 (Fig. 2-4Aii). We further quantified *gerD-gfp* foci by measuring the total fluorescence intensity along the long axis of multiple individual endospores and released spores, and fit the data to a Gaussian distribution (Fig. 2-4B). As a negative control, we again used KGB196 spores (*gerAA-mCherry* Δ*gerD*) that do

not form germinosome foci (Fig 2-4B, dark grey curve). The latter analysis allowed determination of values of σ for these three data sets (Fig. 2-4C), and again, there was no difference between spores in sporangia and released spores but there was a significant difference from the σ value for the GerAA-mCherry signal with *gerD* null spores. The amount of GerD-GFP foci (Fig. 2-4D, black line) and DPA accumulated (Fig. 2-4D, grey line) was also measured at various time-points throughout sporulation of strain KGB213 and plotted as a percent of maximum observed. Consistent with our other sporulation experiments, the maximum level of germinosome foci was observed ~3 h before maximum DPA accumulation was achieved.

GerD-fusion proteins form foci in growing cells. To further examine whether GerD foci can form in cells other than *B. subtilis*, we also expressed GerD-Venus in *E. coli*, with expression from an inducible promoter on a plasmid. We found that GerD-Venus also forms individual foci when expressed in *E. coli* (Fig. 2-5A). Finally, we also tested whether GerD expression in *E. coli* could cause association of a GR protein into GerD foci. Notably, when a GerAC-mCherry fusion protein alone was expressed in *E. coli*, this protein did not form clear foci (Fig 2-5B). However, when GerD was also expressed, the fluorescence pattern from the GerAC-mCherry protein changed significantly, as GerAC-mCherry formed clear foci (Fig. 2-5B, arrows). We verified expression of GerD-Venus and GerAC-mCherry fusion proteins in *E. coli* via Western blot analysis (data not shown).

2-5 DISCUSSION

In this work, the use of fluorescently labeled germination proteins revealed that the germinosome appears in sporulation as discrete foci when fluorescence from these fusion proteins is detected, and essentially in parallel with synthesis of germination proteins as monitored by measuring expression of the *sspA* gene that is expressed in parallel with *gerD* and GR genes (52,98,107). Invariably this was ~ 3 h before spore core compaction and DPA accumulation. This work then strongly indicates that the germinosome forms in parallel with synthesis of its germination protein components, GRs and GerD, with GerD being crucial for germinosome formation, since even in sporulation, GR proteins were not associated with a germinosome when GerD was absent. However, it is important to note that in measuring β-galactosidase accumulation during sporulation, it is a spore population that is being assayed. Consequently, the rather broad β-galactosidase accumulation curves seen may be due to the large heterogeneity between individual sporulating cells in the population, and the expression of sporulating genes in individual developing spores most likely takes place in a shorter time period than in the population as a whole. Additionally, GFP and mCherry proteins have a maturation time ranging from 6-30 min (64,90), which may be why germinosome appearance seems to be slightly after β-galactosidase activity is detected. Clearly, however, the maximum percentage of germinosome foci observed was consistently ~3 h before maximum CaDPA accumulation, an event that occurs via a channel composed of the SpoVA proteins (44,87). The SpoVA proteins are also synthesized at the same time as the germination proteins but are not associated with the germinosome (30,107).

The demonstration that a *gerD-gfp* fusion strain that lacks all the germinant receptors still forms fluorescent foci in sporulating *B. subtilis* indicates that GerD is capable of self associating independently of the GRs. This is consistent with the observation that it self associates in the absence of GRs in dormant spores (30). The crystal structure of 2/3rd of *Geobacillus stearothermophilus* GerD was recently solved; the protein forms a largely hydrophilic rod-like trimer with a hydrophobic lipid anchor, but also shows a trimeric structure capable of self-associating to form higher order structures (46). These results suggest that GerD foci may be able to self-associate to form a higher order structure that acts as a scaffold on which GRs can assemble to form the germinosome, and perhaps this scaffold facilitates signal transduction events in spore germination. Unfortunately, *in vitro* affinity pull-down experiments with purified GerD lacking only the N-terminal signal peptide show that GerD does not associate with GerBC (46), perhaps because GerD does not interact with the GRs' C subunit, or that the interactions facilitated by the germinosome only occur within a membrane.

That GerD can self-associate even in cells that do not have a membrane like that in dormant spores was also shown by formation of foci of GerD-Venus in growing cells of *E. coli*. It was somewhat surprising that multiple GerD-fusion protein foci were seen in growing cells, in contrast to the formation of only one GerD focus in > 90% of dormant *B. subtilis* spores, although some spores do contain two GerD foci (30). Reasons for this difference in numbers of GerD foci formed in spores and growing cells are not clear, but could be due to differences in sizes of these two cell types or differences in levels of GerD-fusion proteins. Notably, when GerAC-mCherry was expressed in growing *E. coli* cells no foci were seen, but only diffuse fluorescence (Fig. 5B). However, when GerD

was coexpressed with GerAC-mCherry in growing *E. coli*, the GerAC-mCherry protein formed foci, analogous to the formation of foci in developing *B. subtilis* spores. This observation strongly supports the ideas that: i) the spore IM alone is not essential for germinosome formation; and ii) GerD self-association creates a germinosome framework on which GRs can assemble.

In sporulating *B. subtilis*, the spore IM is compressed significantly late in sporulation (12,108), and even though the germinosome forms well before this event in sporulation, the IM could well play a role in maintaining this protein complex. Our data suggest that when σ^G becomes activated after endospore engulfment is complete (45,68) and the germination proteins are synthesized, the germinosome forms almost immediately. These events occur well before the IM compresses, and the developing spore matures into its dormant state (37). Similarly, when spores germinate, and the spore core expands and IM lipid mobility is restored, the germinosome does not immediately disperse, but only ~ 1 h after germination is initiated (102). This is further evidence that the novel properties of the dormant spore IM are not essential for germinosome formation and maintenance.

Many questions still remain about the germinosome, specifically the interactions that hold proteins together in this complex. While it appears that GerD self-associates into discrete foci, whether in developing spores or growing cells, the same is not as clear for the GRs, as they absolutely require GerD to properly form the germinosome. Perhaps GerD forms a stable scaffold on which the GRs form, and GRs themselves exist in a transient interacting state. These transient protein interactions, or "soft wired signaling concepts" imply that signaling proteins translocate and have reversible binding

interactions as part of their overall signaling pathway (63,100). It is also possible that the GRs exist in two different conformations, one receptive to interacting with GerD and other GRs in dormant spores and another in germinating spores not receptive to protein interactions. There is no direct evidence for this scenario, however there is evidence for cooperation among the GRs (34,94) and membrane proteins existing in two conformations (95,96).

Thus, we propose a germinosome model where GerD serves as a "snapshot" protein: 1) in sporulating *B. subtilis*, soon after protein synthesis, GerD self associates and forms the foundation for the GRs to associate with; 2) the colocalized proteins remain fixed in place in largely immobile dormant spore inner membrane; 3) upon receiving nutrient signals from the environment this signal is transduced via the germinosome and spore germination commences; 4) levels of GerD decrease rapidly, spore IM expand ~2 fold, and spore IM lipid mobility is restored, all of which facilitates the dispersion of the germinosome. In this model, the function of GerD is to create the scaffold for the germinosome to form, and to facilitate whatever signal triggers CaDPA release from the spore core. This occurs in a very short time period, therefore GerD is only required for a snapshot in time, before this protein ultimately becomes degraded in germinating spores (103). From this work, it is clear that further experimentation is needed to understand the germinosome, specifically the protein-protein interactions within the germinosome.

ACKNOWLEDGEMENTS

We thank Keren Griffiths for creating strain KGB123. This work was supported by a Department of Defense Multi-disciplinary University Research Initiative through the U.S. Army Research Laboratory and the U.S. Army Research Office under contract number W911F-09-1-0286 (PS/JY/AC).

Table 2-1. *B. subtilis* strains used*

Strain	Genotype and phenotype	Source (reference)
FB41	PS832 Δ*gerB* Sp^r	(16)
PS533	wild-type pUB110 Km^r	(81)
PS3418	PS832 Δ*gerK* Tc^r	(37)
PS3609	PS832 Δ*gerA* Nm^r	(37)
PS4150	PS832 Δ*gerE* Δ*cotE* Sp^r Tc^r	(28)
KGB73	PS4150 *gerD-gfp* Km^r	(30)
KGB80	PS4150 *gerKB-mCherry gerD-gfp* Cm^r Km^r	(30)
KGB114	PS4150 *amyE::gerAA-mCherry* Cm^r	(30)
KGB123	PS4150 *gerD-gfp sspA-lacZ* Km^r Cm^r	(Keren Griffiths)
KGB171	PS4150 Δ*gerD* Cm^r	(Keren Griffiths)
KGB196	PS4150 *gerAA-mCherry* Δ*gerD* Km^r Cm^r	(30)
KGB213	PS4150 *gerD-gfp* Δ*gerA* Δ*gerB* Δ*gerK* Km^r MLS^r	(30)

*Abbreviations used are resistance to: Cm^r, chloramphenicol (10 μg/ml); Km^r, kanamycin (10 μg/ml); MLS^r, erythromycin (1 μg/ml) and lincomycin (25 μg/ml); Sp^r, spectinomycin (100 μg/ml); Nm^r neomycin (100μg/ml); and Tc^r, tetracycline (10 μg/ml).

Table 2-2. *E. coli* K12 strains used*

Plasmid carried	Genotype and phenotype	Source
pQY4	p*Lac-gerD-venus*	This study
pQY96	p*BAD-gerAC-mcherry*	This study
pJQ61.3	p*BAD-gerAC-mcherry-gerD*	This study

* Plasmids were generated as described in Methods.

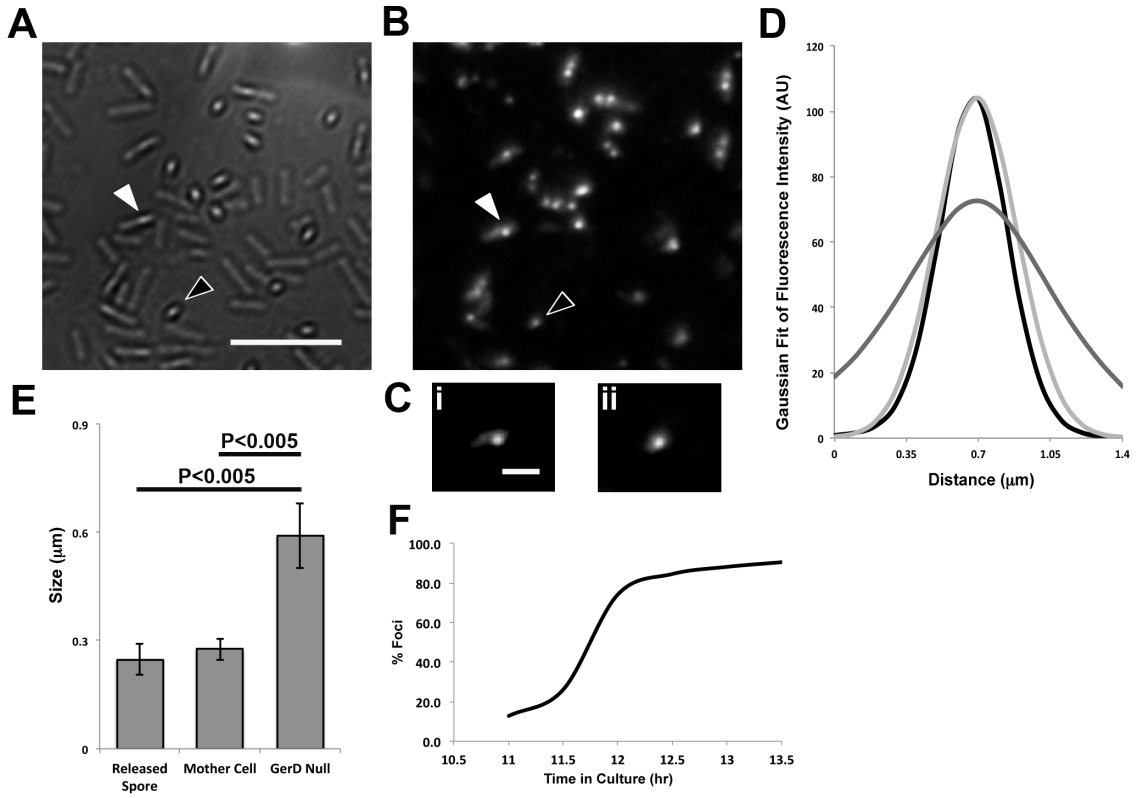

Fig. 2-1A-E. DIC and fluorescence microscopic analysis of sporulating cells of strain KGB114 (PS4150 *gerAA-mCherry*). A) DIC and (B) fluorescence images of spore populations after 12.5 h in culture as described in Methods. The scale bar in (A) is 5 μm and the image in (B) is at the same magnification. The white arrow in (A) and (B) indicates a developing spore within a mother cell, and the black arrow indicates a released spore. (C) 7x magnification of areas marked in panel (B): (i) a spore within a mother cell (white arrow), and (ii) a released spore (black arrow). Scale bar in (i) is 1 μm and panels (i) and (ii) are the same magnification. (D) Average Gaussian fit of fluorescence intensity along the long axis of 20 spores within a mother cell (black curve), 20 released spores (light grey curve), and 20 released KGB196 (*gerAA-mCherry* Δ*gerD*) spores (dark grey curve). (E) Changes in (σ) of the Gaussian distribution from (D) in

KGB114 released, KGB114 mother cell contained, and released Δ*gerD* (KGB196) spores. Error bars represent one standard deviation and P-values determined by the students two-tailed T-test are given above graph. (F) The percentage of the total spore population (both released and within a mother cell) that has a germinosome focus as a function of time in culture. The maximum percentage of spores with clear germinosome foci was ~ 85%, as seen previously (6).

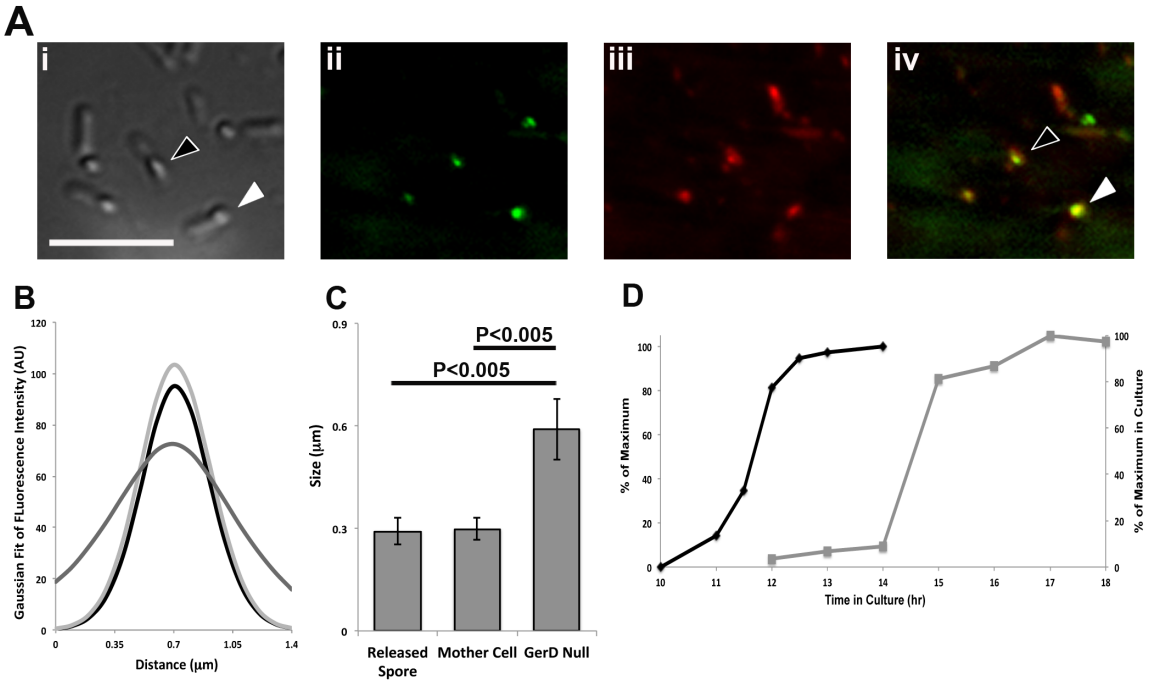

Fig. 2-2A-D. DIC and fluorescence microscopic analysis of sporulating cells of strain KGB80 (PS4150 *gerKB-mCherry gerD-gfp*). (A) DIC image (i), fluorescence image of GFP (ii), mCherry (iii), and GFP/mCherry overlay (iv) after 12.5 h in culture. The scale bar in panel (Ai) is 5 μm, and panels (i-iv) are at the same magnification. In (i) and (iv), the white arrow indicates a spore contained within a mother cell, and the black arrow indicates a released spore. (B) Gaussian fit of overlay fluorescence intensity along the long axis of 20 spores within a mother cell (black curve), 20 released spores (light grey curve), and 20 released KGB196 (*gerAA-mCherry* Δ*gerD*) spores (dark grey curve). (C) Changes in (σ) of Gaussian distribution from (B) in KGB80 released, KGB80 mother cell contained, and released Δ*gerD* (KGB196) spores. Error bars represent one standard deviation and P-values determined by students two-tailed T-test are given above graph. (D) Plot of levels of germinosome foci (black line) and DPA accumulated (grey line) as percentages of maximum levels observed as a function of time in culture.

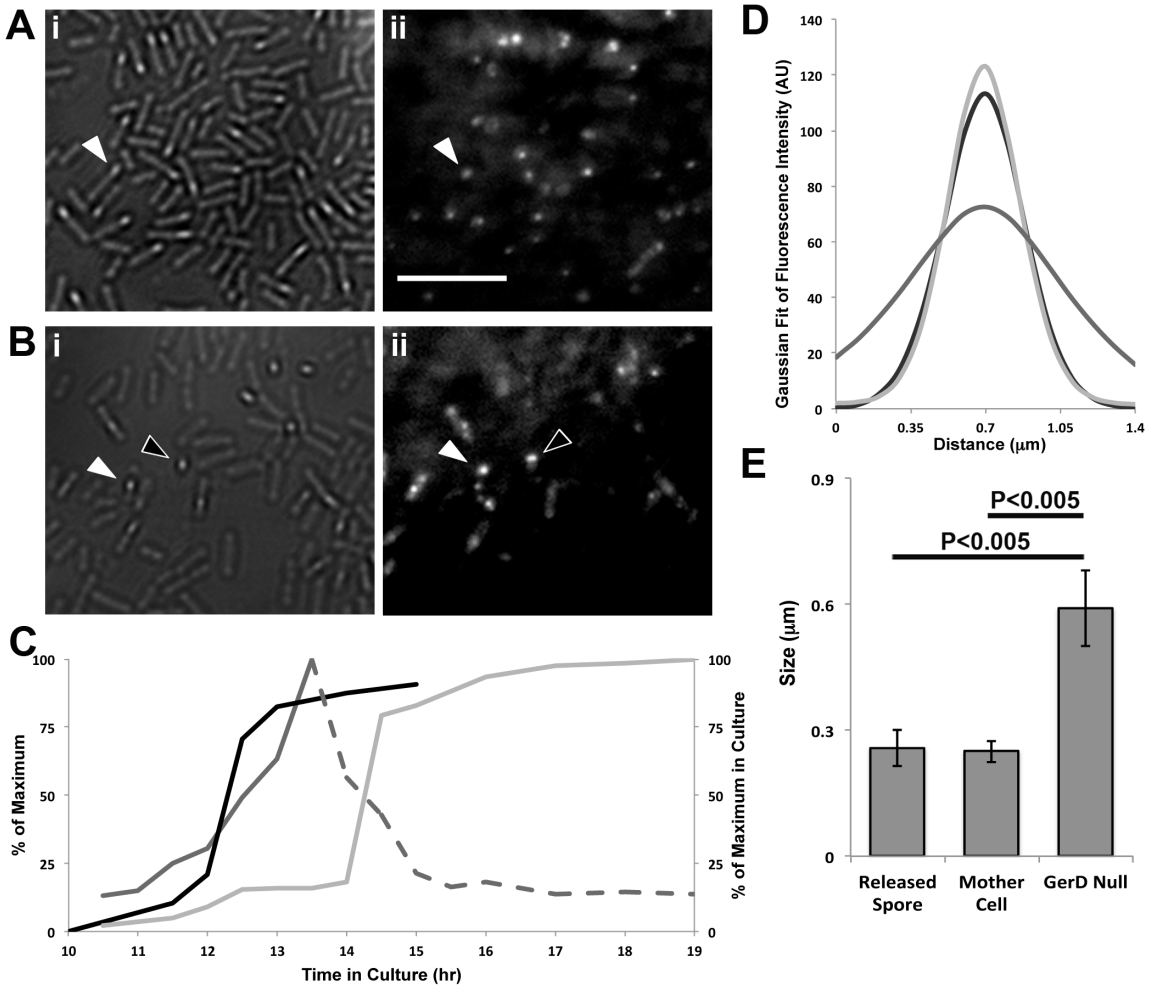

Fig. 2-3A-E. DIC and fluorescence microscopy of sporulating cells of strain KGB123 (PS4150 *gerD-gfp sspA-lacZ*) and synthesis of β-galactosidase. (A) DIC (i) and fluorescence (ii) images of spore populations after 11.5 h in culture. The scale bar in panel (ii) is 5 μm and magnifications in (i) and (ii) are identical. (B) DIC (i) and fluorescence (ii) images of spore populations after 13.5 hours in culture. Panels in (Bi-ii) are at the same magnification as panels in (Ai-ii). The white arrow in (A) and (B) indicates a spore within a mother cell and the black arrow in (B) indicates a released spore. (C) % of spores with a germinosome focus (black line), β-galactosidase specific activity (dark grey line, dark grey dotted line), and DPA accumulation (light grey line) as

percentages of maximum levels observed as a function of time in culture. (D) Gaussian fit of fluorescence intensity along the long axis of 20 spores within a mother cell (black curve), 20 released spores (light grey curve), and 20 released KGB196 (*gerAA-mCherry* Δ*gerD*) spores (dark grey curve). (E) Changes in (σ) of Gaussian distribution from (D) in KGB123 released, KG123 mother cell contained, and released (KGB196) spores. Error bars represent one standard deviation and P-values determined by students two-tailed T-test are given above the graph.

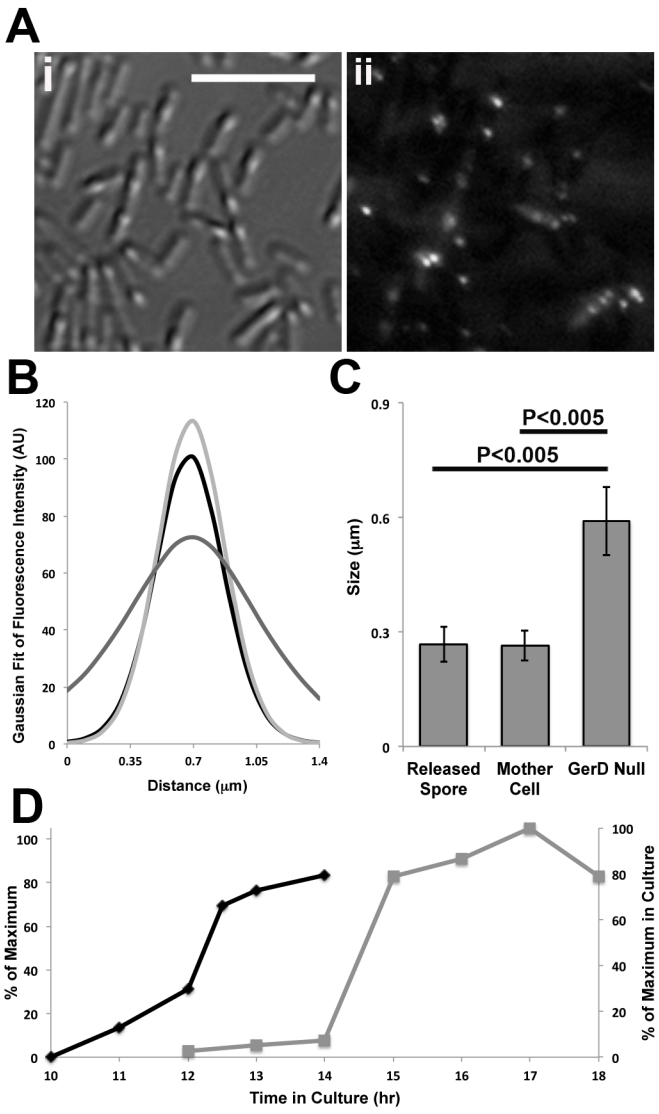

Fig. 2-4A-D. DIC and fluorescence microscopic analysis of sporulating KGB213 (PS4150 *gerD-gfp* Δ*gerA* Δ*gerB* Δ*gerK*). A) DIC (i) and fluorescence (ii) images of endospore populations after 12 h of sporulation. The scare bar in (i) is 5 μm and (i) and (ii) are at the same magnification. (B) Average Gaussian fit of fluorescence intensity along the long axis of 20 spores within a mother cell (black curve), 20 released spores (light grey curve), and 20 released KGB196 (*gerAA-mCherry* Δ*gerD*) spores (dark grey curve). (C) Graph of change in (σ) of Gaussian distribution from (B) in KGB213

released, KG213 mother cell contained, and released KGB196 spores. Error bars represent one standard deviation and P-values determined by students two-tailed T-test are given above the graph. (D) Plot of levels of GerD-GFP foci (black line) and DPA accumulated (grey line) as percentages of maximum levels observed as a function of time in sporulation.

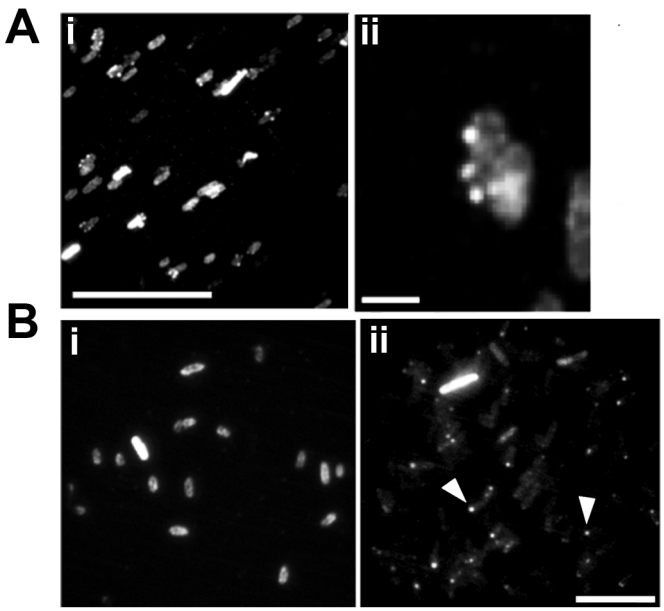

Fig. 2-5A-D. DIC and fluorescence microscopy of *E. coli* cells expressing germination proteins. A) Fluorescence images of GerD-Venus in *E. coli*, scale bar in (i) is 5 μm and (ii) is 1 μm. B) Fluorescence images of GerAC-mCherry localization, without GerD expression (i) and with GerD expression (ii). Scale bar in panel (ii) is 5 μm and panels (i-ii) are at the same magnification.

CHAPTER 3

GERMINSOME DYNAMICS IN SPORE GERMINATION

Analysis of the dynamics of a *Bacillus subtilis* spore germination protein complex during spore germination and outgrowth

Anthony J. Troiano Jr.[1], Jingqiao Zhang[2], Ann E. Cowan[1], Ji Yu[2] and Peter Setlow[1]*

Departments of [1]Molecular Biology and Biophysics, and [2]Cell Biology

University of Connecticut Health Center

Farmington, CT 06030

Running title: Changes in the germinosome during spore germination

Key words: *Bacillus*, spores, spore germination, germinant receptors, GerD, germinosome

*Corresponding author

Address: Department of Molecular Biology and Biophysics, University of Connecticut Health Center, Farmington, CT 06030-3305

Phone: 860-679-2607

Fax: 860-679-2308

Email: setlow@nso2.uchc.edu

CHAPTER 3 - CONTRIBUTIONS

The work performed in chapter three was led by Anthony J. Troiano Jr., including all spore preparation; all fluorescent strains used were previously created in Peter Setlow's laboratory by Keren Griffiths. Isolation of germinating and outgrowing spore populations, spore lysate preparation, and Western blot analysis was done by Anthony J. Troiano Jr. All microscopy experiments were performed in Ji Yu's laboratory on his custom Nikon epifluorescence microscope, under the supervision of Jingqiao Zhang and Ann E. Cowan. Subsequent microscopy analysis and germinosome quantitation was executed by Anthony J. Troiano Jr., under the supervision of Ann E. Cowan. Analysis of fluorescence distributions via Guassian curve fitting, as well as ImageJ and photoshop analysis was done by Ann E Cowan and Anthony J. Troiano Jr. The writing in the following chapter was primarily done by Anthony J. Troiano Jr. under the supervision of Peter Setlow.

3-1 Abstract

Germination of *Bacillus subtilis* spores is normally initiated when nutrients from the environment interact with germinant receptors (GRs) in spores' inner membrane (IM) in which most of the lipids are immobile. GRs and another germination protein, GerD, co-localize in dormant spores' IM in a small focus termed the "germinosome", and this co-localization or focus formation is dependent upon GerD that is also essential for rapid GR-dependent spore germination. To determine the fate of the germinosome and germination proteins in spore germination and outgrowth we employed differential interference microscopy and epifluorescence microscopy to track germinating spores with fluorescent fusions to germination proteins, and used western blot analyses to measure germination protein levels. We found that after initiating spore germination, the germinosome foci ultimately changed into larger disperse patterns, with ≥ 75% of spore populations displaying this pattern in spores germinated for one hr, although >80% of spores germinated for 30 min retained the germinosome foci. Western blot analysis revealed that levels of GR proteins and the SpoVA proteins essential for dipicolinic acid release changed minimally during this period, although GerD levels decreased ~ 50% within 15 min in germinated spores. Since the dispersion of the germinosome during germination was slower than the decrease in GerD, either germinosome stability is not compromised by ~ 2-fold decreases in GerD level, or other factors such as restoration of rapid IM lipid mobility are also significant in germinosome dispersion as spore germination proceeds.

3-2 Introduction

Spores of *Bacillus subtilis* are metabolically dormant and resistant to harsh environmental conditions, allowing them to survive for many years (84). However, the presence of specific nutrients triggers the process of germination in which spores lose their dormancy and resistance and then outgrow into vegetative cells. Normally, for germination to occur nutrients must cross the coat, outer membrane, cortex, and germ cell wall of the dormant spore to reach nutrient germinant receptors (GRs) located in spore's inner membrane (IM) (36,59,84). Lipid molecules in the *B. subtilis* spore IM are largely (~ 70%) immobile, but upon completion of spore germination the volume encompassed by the IM expands ~ 1.5 fold and the amount of the immobile lipid fraction decreases to ~ 25%, similar to the value in vegetative cells, all in the absence of detectable ATP synthesis (12). Binding of specific germinants to their cognate GRs leads to release of the spore core's large store (~ 25% of core dry weight) of dipicolinic acid (DPA) chelated to divalent cations, mostly Ca^{2+} (CaDPA); CaDPA release is accompanied by some water uptake into the core and some loss of spore resistance. CaDPA release also triggers degradation of the spore's peptidoglycan (PG) cortex by cortex-lytic enzymes (CLEs), allowing for core expansion, further core water uptake and completion of germination, and ultimately outgrowth to generate a vegetative cell (84).

Three functional GRs have been identified in *B. subtilis* spores, GerA, GerB, and GerK, each encoded by a homologous tricistronic operon producing two polytopic integral transmembrane proteins (A and B subunits) and a peripheral membrane lipoprotein (C subunit). Other spore IM proteins involved in germination include GerD, a lipoprotein involved in GR-dependent germination, and the 7 SpoVA proteins, most of

which are integral membrane proteins involved in CaDPA movement into and out of the spore in sporulation and germination, respectively (45,68,107). It is known that some GRs cooperate during spore germination, but overall the mechanisms for signal transduction in spore germination are unknown and this is one of the biggest gaps in our understanding of spore germination (84,112).

A recent study showed that GerD and all GRs in *B. subtilis* spores colocalize in a small focus in spores' IM in a structure termed the germinosome (30). Upon deletion of *gerD*, the GRs fail to colocalize and instead are diffusely distributed throughout the IM, suggesting that GerD facilitates germinosome formation, and GerD forms a small IM focus in dormant spores even in the absence of all GRs (30). The loss of GerD also causes a significant decrease in spore germination rates with nutrient germinants, furthering the significance of the germinosome and GerD in spore germination (65). Spores lacking GerD germinate normally with non-nutrient germinants that bypass the GRs, suggesting that GerD is required for efficient signal transduction from the nutrient-GR complex; however, the exact signaling mechanism remains unknown (65). The crystal structure of 2/3rd of *Geobacillus stearothermophilus* GerD was solved recently, and the protein forms a rod-like trimer that is largely hydrophilic with a hydrophobic lipid anchor (47). Interestingly, a previous study as well as very recent work indicate that levels of GerD decrease markedly in the IM fraction from germinating and early outgrowing spores, suggesting that the protein becomes soluble or is degraded during this period (9,66).

The mechanism by which GerD interacts with the germinosome is unknown and our knowledge of this protein complex is limited only to its features in dormant spores

(30). If GerD does act as a scaffold that GRs use to assemble into the germinosome, then as GerD levels decrease in germinating/early outgrowing spores, the scaffold for the germinosome might erode away and as a result this complex might disassociate in germination/early outgrowth. The aim of this study was to test this hypothesis by examining the dynamics of the germinosome as well as various germination proteins during the germination and outgrowth of *B. subtilis* spores. Studying the fates of the germinosome, GR subunits and GerD during spore germination and outgrowth might further the understanding of these processes and perhaps provide clues to how signal transduction works in spore germination.

3-3 MATERIALS AND METHODS

***B. subtilis* strains and spore preparation.** *B. subtilis* strains used for this work are listed in Table 3-1 and are isogenic with strain PS832, a prototrophic 168 laboratory strain. The fluorescent fusion strains are all isogenic derivatives of PS4150, derived from PS832 and lacking two genes essential for spore coat assembly, *cotE* and *gerE*. Loss of these two genes results in a greatly reduced autofluoresence background due to the absence of most coat proteins in the PS4150 spores, allowing visualization of fluorescence from GFP derivatives fused to germination proteins. The fusion strains are: i) KGB72 with an *mCherry* sequence fused to the C-terminal coding end of the *gerKB* gene at the *gerK* locus and with a wild-type *gerKB* gene that is most likely not transcribed; ii) KGB73 with a *gfp* sequence fused to the C-terminal coding end of the *gerD* gene at the *gerD* locus and that retains an expressed wild-type *gerD* gene; iii) KGB80 with the *gerKB-mCherry* fusion in strain KGB72 and the *gerD-gfp* fusion in strain KGB73; iv) KGB94, which is strain KGB73 that has been transformed to Cm^r using chromosomal DNA from strain PS2307 (Δ*cwlD*) that carries a deletion of the *cwlD* gene essential for modification of spore cortex PG such that CLEs can recognize and degrade the cortex during stage II of spore germination (29,74); and v) KGB114 with a *gerAA-mCherry* sequence inserted at the *amyE* locus downstream of the native promoter for the *gerA* operon encoding the GerA GR. Spores of all fusion strains germinate relatively normally with nutrients in the absence of endogenously expressed protein, indicating that the fusion proteins are functional (30).

Spores of *B. subtilis* strains were prepared at 37°C on 2x Schaeffer's-glucose agar plates without antibiotics, and spores were incubated, harvested, and cleaned as described

previously (56). All spores in this work were free (>98%) of growing or sporulating cells, germinated spores, and cell debris, and spores were stored at 4°C protected from light.

Spore germination and outgrowth. For western blot analysis, spores at an optical density at 600 nm (OD_{600}) of 125 in water were heat activated at 75°C for 30 min and cooled on ice for ~ 15 min. Heat activated spores were germinated at an OD_{600} of ~ 1.5 at 37°C in 200 ml of 10 mM L-valine plus 25 mM K-Hepes buffer (pH 7.4). Spore germination kinetics were determined by measuring the OD_{600} of germinating cultures, and 65 ml samples were harvested by centrifugation (10 min; 12,000xg) after 15, 60, and 120 min of germination. The pellets from these samples were washed in phosphate buffered saline (PBS) (50 mM NaH_2PO_4, 150 mM NaCl [pH 7.2]), suspended in 5 ml PBS and washed 3x with PBS by centrifugation at 12,000xg. The final spores were suspended in 200 μl 20% Histodenz™ (Sigma-Aldrich Corporation, St. Louis, MO), loaded on a Histodenz density cushion (1 ml of 50% Histodenz) and centrifuged for 15 min at 15,000xg to separate germinated spores from non-germinated spores (27). Germinated spores were isolated by pipetting off the 20% Histodenz layer, diluted in 1 ml PBS, cleaned by centrifugation at 12,000xg for 10 min and washing the pellet five times with PBS to remove Histodenz. Germinated spore samples were suspended in 250 μl PBS and stored at -80°C.

To isolate outgrown spores, heat-activated spores were germinated at an OD_{600} of 1 as described above. After 2 hr of germination the spores were run on a Histodenz gradient to separate germinated and dormant spores, and germinated spores were isolated and washed as described above. These germinated spores were suspended in 15 ml of LB

medium (56) at an OD_{600} of 0.5. Immediately upon suspension in LB medium, a 5 ml sample was harvested by centrifugation (15 min; 12,000xg); this sample served as the 2 hr germination sample in outgrowth experiments. The remaining 10 ml of germinated spores were incubated at 37°C with vigorous shaking. Samples (5 ml) of these cultures were harvested by centrifugation (15 min; 12,000xg) at an OD_{600} of 1 and 2 and microscopic analysis confirmed that the germinated spores had outgrown into vegetative cells. All three samples were washed with PBS three times to remove growth medium, suspended in 0.5 ml PBS, and stored at -80°C.

Preparation of spore lysate and Western blot analysis. Dormant, germinating, and outgrowing/growing spore samples prepared and harvested as described above were treated with lysozyme (0.5 mg/mL) in TEP buffer (50 mM Tris-HCl [pH 7.4], 5 mM EDTA, 1 mM phenylmethylsulfonyl fluoride, 1% Triton X-100) for 5 min at 37°C and then 20 min on ice. After incubation, the lysed samples were sonicated on ice with 100 mg of glass beads for five 15 sec periods, with 30 sec intervals between sonication periods. After sonication, samples were made to 1% SDS and 150 mM 2-mercaptoethanol and incubated for 2 h at 23°C (92). The samples were then bath sonicated for 2 min, centrifuged for 5 min at 16,000xg, and the supernatant fluid collected was termed the total lysate fraction (L). The pellet fractions were suspended in TEP buffer containing 1% SDS and 150 mM 2-mercaptoethanol, bath sonicated for 2 min, centrifuged at 16,000xg, and the resulting supernatant fluid was termed the washed lysate fraction. Invariably, levels of germination proteins in this washed lysate fraction were < 10% of the levels found in the L fraction (data not shown).

In each experiment, equal aliquots from the same amounts of various spore fractions were run on SDS-polyacrylamide (12%) gel electrophoresis (PAGE), proteins transferred to polyvinylidene difluoride (PVDF) membranes and membranes probed with antisera specific for various germination proteins as described previously (76,93,94). In some experiments, after the use of one antiserum, the PVDF membranes were stripped with Restore Western blot stripping buffer (Thermo Scientific, Rockford, IL) for 15-20 min at 37°C and then probed again with antiserum against another germination protein. ImageJ software was used to compare the intensities of protein bands obtained from western blots on X-ray film, which were further compared to bands from western blot analysis of serial dilutions of germinating spore samples.

Microscopy. For fluorescence microscopy of germinating spores, dormant spores suspended in water at an OD_{600} of ~35 were heat activated for 30 min at 75°C and then cooled on ice for 15 min. The heat-activated spores (10 μl) were spread on 0.1% poly-lysine-coated glass bottom culture dishes (MatTek, Ashland, MA), and to germinate the spores, a mixture with final concentrations of 10 mM L-valine - 25 mM K-Hepes buffer (pH 7.4) was added. Germination on the microscope platform was at 37°C using a heated slide chamber. Epifluorescence and differential interference microcopy (DIC) images were taken of the dormant spores at various germination times as described previously (30), and images were processed using ImageJ and Adobe Photoshop software. Enlarged images were scaled at 300 pixels/inch using a bicubic function. Due to the relatively weak signal to noise ratio in the spores, we summed 30-50 consecutive fluorescent images at each time point with an acquisition time of ~70 msec. Increasing the number of images taken or increasing the acquisition time led to significant photobleaching. Images

used in subsequent analysis were generated as described previously (30). In determining colocalization of the signal from two fluorescent proteins, if the maximum intensities of the two signals were ≤ 1 pixel apart (corresponding to 160 nm), then they were scored as colocalized, since the positions of the mCherry and GFP foci can be partially shifted because of the signal noise and the wavefront alteration caused by changing of dichroic mirrors (30). Fluorescence distribution curves along the long axis of spores were generated as described previously (30). Plots of σ, or the width of the Gaussian distribution at (1/e) the maximum fluorescence intensity, were generated, and P-values calculated using the student's two-tailed t-test.

3-4 RESULTS

Levels of GR subunits in the L fraction from germinating wild-type spores. Since the fate of all GR subunits in spore germination and outgrowth has not been thoroughly studied (9), we first examined levels of GR subunits in dormant and germinating spores to determine how long GR subunits persist following initiation of germination. GRs localize to the IM in spores (30,36,57,84), but recent work found that only ~ 10% of GR subunits are found in isolated IM, since ~ 90% sediment upon low speed centrifugation of a spore lysate made without SDS and 2-mercaptoethanol and ~ 90% of the IM lipids also sediment upon the same low speed centrifugation (92). Consequently, to ensure we analyzed all GR subunits in spores, we added SDS plus mercaptoethanol to spore lysates and incubated for ~ 2 hr at 23°C prior to centrifugation, conditions that give ≥ 90% of germination proteins in soluble form (93). Western blot analysis of these samples with antisera against GR subunits (Fig. 3-1) showed that in wild-type spores, the levels of all GR subunit proteins were essentially the same in dormant and germinating spores, with the exception of GerBC and GerKA. GerBC band intensities decreased slightly in germination, and GerKA levels decreased more significantly (Fig. 3-1), although this was not seen in all experiments (data not shown; and see below). However, since significant levels of GR subunits as well as GerD (see below) persisted even after 2 hr of germination, it is certainly possible that a germinosome could persist in germinating spores for extended periods.

Dynamics of GerD and SpoVA proteins in dormant and germinating wild-type spores. As noted above, GerD plays an important role in spore germination, likely because this protein is essential for the formation of the germinosome in dormant spores.

Previous studies suggested that levels of GerD in inner spore membrane fractions decrease in germination (9,65), but did not study what happens to GerD in a total spore lysate. When probing the L fraction of wild-type spores with antisera against GerD, we found the levels of this protein decreased significantly in germination, more than 50% after 15 min (Fig. 3-1; and see below). We confirmed this finding by Western blotting using serial dilutions and through ImageJ density analysis (data not shown). This suggests that initially the germinosome could remain intact in germinating spores, but as GerD levels decrease the germinosome might disperse in germinating/outgrowing spores.

Levels of some members of another important group of proteins involved in germination, the SpoVA proteins, were also examined in dormant and germinating spores. These proteins are not found in the germinosome (30), but play an important role in the overall germination process by facilitating movement of CaDPA out of the spore core (45,68). Like GerD and total GRs, the SpoVA proteins are present in the IM at several thousand molecules per spore (93,94). Western blots of the L fraction of wild-type spores with antisera against SpoVAD or SpoVAEA found no significant differences in the levels of these proteins between dormant and germinating spores (Fig. 3-1).

Germinosome foci disperse during germination of spores with single fluorescent fusions. To study the germinosome in *B. subtilis* spore germination, we first examined spores with single fluorescent fusions to germination proteins to determine if these individual germination proteins exhibited any change in their distribution or location during germination. Specifically, we examined KGB73 (PS4150 *gerD-gfp*) and KGB114 (PS4150 *gerAA-mCherry*) spores using DIC and fluorescence microscopy, analyzing both dormant and 2 hr germinated spores. Germinated spores can be distinguished from

dormant spores by the large drop in their refractive index due to CaDPA release from the spore core and its replacement by water, as well as core swelling and further water uptake following cortex PG hydrolysis (84,108) (Fig. 3-2Ai, 3-3Ai). Spores of both KGB73 (Fig. 3-2Aii) and KGB114 (Fig. 3-3Aii), exhibited similar fluorescence changes after 2 hr of germination; while dormant spores exhibited distinct fluorescent foci, germinated spores exhibited a more dispersed fluorescence signal and a lower peak fluorescence intensity (Fig. 3-2Bii, 3-3Bii).

In order to compare spores' fluorescence quantitatively, the fluorescence intensities of 20 individual spores, when dormant and then after 2 hr of germination, were measured along their long axis. The full width at half maximal intensity for dormant KGB114 spores was ~ 300 nm (data not shown), as seen previously (30), indicative of the maximum germinosome size and the resolution limit of the microscope. When these fluorescence intensities were fit to a Gaussian distribution and averaged (Fig. 3-2C, 3-3C; black curves), the resulting curves were similar to those seen previously for dormant spores with comparable fluorescent fusions (30). However, there was a significant change in signal distribution after 2 hr of germination (Fig. 3-2C, 3-3C; grey curves). To compare the change in Gaussian distributions between dormant and 2 hr germinated spores, we determined σ, or the width of the curve at (1/e) of the maximum fluorescence intensity, at both time points (Fig. 3-2D, 3-3D). For each fluorescent fusion, σ increased notably in 2 hr germinated spores, and this change was statistically significant (Fig. 3-2D, 3-3D). This change is in agreement with our fluorescence imaging that indicated that the germinosome becomes disperse and the fluorescence distribution broadens as the spore germinates. Thus, even though levels of GerD in wild-type spores decreased as much as

50% 15-min post germinant addition, GerD-GFP and GerAA-mCherry fluorescence was still detectable in spores 2 hr post-germinant addition, however, not in discrete foci but in a more disperse distribution in which the average maximum fluorescence intensity decreased 2 to 3-fold (Fig. 3-2C, 3-3C; and see below).

Germinosome foci disperse during germination of spores with two fluorescent fusions. To further understand the fate of the germinosome in *B. subtilis* spore germination, dormant and germinating KGB80 (PS4150 *gerKB-mCherry gerD-gfp*) spores were also examined using DIC and fluorescence microscopy. Images were taken before a nutrient germinant was added (dormant), and 1 and 2 hr post germinant addition (Fig. 3-4A). Time-lapse microscopy of these spores showed that upon germination, the germinosome again displayed two different appearances: discrete foci (Fig 3-4Ci) in which GRs and GerD are colocalized as seen previously in dormant spores (30), and a more diffuse signal in which GRs and GerD are dispersed (Fig. 3-4Cii). However, in some germinating spores, ~ 20% after 2 hr of germination, no fluorescence signal was seen (see below). Loss of fluorescence signal due to photobleaching was not apparent (Fig. 3-4Axii, asterisk), and this was confirmed with control photobleaching experiments (data not shown). KGB80 spores germinated effectively in glass bottom dishes, with ~75% of spores germinated after 2 hr (see below), although this was slower than in solution (data not shown). In this work, we define the time of the completion of the fall in germinating spores' DIC intensity due to complete CaDPA release as well as completion of cortex hydrolysis and core swelling as T_{lys} (25). Spores with a T_{lys} of < 1 hr (Fig. 3-4A, black arrows) as well as those with a $T_{lys} \geq 1$ hr (Figure 3-4A, white arrows) displayed similar dispersed germinosome appearance, suggesting that

germinosome foci remain intact for less than an hour following initiation of spore germination and then disperse.

To further quantitate germinosome dispersion in germinating spores, the total fluorescence intensity along multiple individual dormant spores' long axis and in these same spores after 1 and 2 hr of germination was measured, and the data were fit to a Gaussian distribution and averaged (Fig. 3-4B). The latter analysis allowed determination of values for σ for these three data sets (Fig. 3-4D). As was the case with spores with single fluorescent fusions, there were marked decreases in peak fluorescence intensity (Fig. 3-4B) and significant increases in the value for σ (Fig. 3-4D) as germination of spores with the two fluorescent fusions proceeded. However, the maximum σ value of 600 nm in the 2 hr germinated spores was still smaller that that of the entire spores, consistent with the fluorescent proteins remaining in the IM but being dispersed.

Levels of GR subunits and GerD in L fractions of dormant and germinating spores with single fluorescent fusions. In order to prove that the changes in the germinosome appearance described above are not a result of changes in levels of GR proteins, we also examined levels of GR subunits in dormant and germinating KGB73 (PS4150 *gerD-gfp*) and KGB114 (PS4150 *gerAA-mCherry*) spores (Fig. 3-5A,B). As seen with wild-type spores, western blots of L fractions from dormant and germinating KGB73 and KGB114 spores showed that except for GerBC, GR subunit levels changed minimally in germination. It was also notable that the GerD antigen was detected at two molecular weights in western blots of KGB73 spores' L fractions, the normal protein at ~ 18 kDa and GerD-GFP at ~ 47 kDa; surprisingly, while levels of the normal protein decreased during germination, GerD-GFP levels remained unchanged. We confirmed the decrease

in endogenous GerD levels through Western blotting of serial dilutions and ImageJ density analysis. L fractions of KGB114 spores also contained two forms of the GerAA antigen, that of the normal protein of ~ 60 kDa and the ~ 82 kDa GerAA-mCherry, both of which were stable for ~ 2 hr of germination. Since the GR subunits were present throughout germination in these fusion protein strains, we believe changes in their level do not influence the dispersion of the germinosome seen as germination proceeds.

These same western blots showed that levels of SpoVAD and SpoVAEa were also relatively unchanged during germination of KGB73 and KGB114 spores (Fig. 3-5A,B). In contrast, as seen with wild-type spores, levels of normal GerD decreased more than 50% by 15 min post germinant addition and generally even more, and this was confirmed with western blots of serial dilutions of L fractions from spores of both strains (data not shown). However, as noted above, GerD-GFP was detected at ~47 kDa and remained at dormant spore levels throughout germination, indicating that the fusion protein is not degraded or processed during germination. This explains why a GerD-GFP signal could still be seen by fluorescence microscopy 2 hr after germinant addition to KGB73 spores, although not in foci but as a more disperse signal (Fig. 3-2).

Timing of germinosome dispersion during spore germination. While it was clear from analysis of spores germinating for 2 hr that the germinosome ultimately disperses during germination, it was important to determine when this change took place as this might identify germination events correlated with germinosome dispersion. There are two stages in spore germination (84): stage I characterized by CaDPA release, followed by stage II in which cortex PG is degraded by CLEs and the spore core takes up water and expands. Events in these two stages can be examined separately by using spores of strains

that cannot degrade their cortex PG. One such strain lacks the CwlD protein essential for a specific cortex PG modification that allows CLEs to specifically recognize and degrade this modified PG (1,15,19). Spores of a *cwlD* strain go through stage I of germination relatively normally, but further germination events do not take place, including the large decrease in the immobile fraction of IM lipid (4,14). DIC and fluorescence microscopy of KGB94 (PS4150 *gerD-gfp* Δ*cwlD*) spores indicated that > 95% of dormant spores contained fluorescent GFP foci (Table 3-2). Germinated spores of this *cwlD* strain could be identified by their decreased DIC image contrast, although this decrease was not quite as great as in spores that could go through stage II of germination (Fig. 3-6A). Strikingly, almost all the germinated KGB94 spores retained their fluorescent foci even after 2 hr of germination, with no increase in spores with a dispersed germinosome (Fig. 3-6B) (Table 2). Thus events in stage I of germination are not sufficient to trigger germinosome dispersion.

To more precisely determine when the germinosome disperses during spore germination, the germinosome appearance in multiple individual germinating spores carrying fluorescent fusions was determined at various times in germination as well as in dormant spores (Table 3-3). This analysis showed that germinosome dispersion did not become significant until between 15-30 min post germinant addition, with most taking place between 30-60 min after germinant addition. There was also an increasing percentage of spores that had minimal if any fluorescence signal remaining as germination progressed, although this loss in fluorescence signal was not due to photobleaching as noted above.

Levels of germination proteins in outgrowing spores. While levels of GR and SpoVA proteins were relatively constant throughout spore germination, it seemed unlikely that these proteins would be retained indefinitely once spores had outgrown and resumed vegetative growth. To determine when these proteins disappeared following spore germination, wild-type*, gerD-gfp,* and *gerAA-mCherry* spores were germinated, outgrown and grown vegetatively and samples were analyzed by western blots to determine levels of various germination proteins. With germinated spores of these three strains grown to an OD_{600} of 2, the levels of GR subunits, SpoVAEa and SpoVAD decreased 30-85%, 50-60%, and, 50-90%, respectively (Fig. 3-7). Most notably, GerD was at minimal levels if any by an OD_{600} of 1 (Fig. 3-7). With the GerD-GFP fusion strain, we were unable to come to a definitive conclusion about changes in GerD-GFP levels due to high levels of nonspecific binding in the GerD-GFP region of western blots with samples from vegetative cells at an OD_{600} of 1-2 (data not shown). However, GerAA-mCherry levels had decreased ~75% by an OD_{600} of 2 (Fig. 3-7C). The universal decrease in levels of native germination proteins seen in outgrowth and subsequent growth, as well as the complete loss of GerD indicates that as spores complete germination and outgrowth and begin to grow vegetatively, levels of all germination proteins decrease, most notably GerD. Consequently, the germinosome could not persist in wild-type spores once outgrowing spores become growing cells.

3-5 DISCUSSION

How signals are transferred from the GRs to downstream signaling molecules in *B. subtilis* spore germination remains unknown. In dormant spores, germination proteins coalesce into the germinosome, and formation of this multiprotein complex is dependent on the accessory germination protein GerD (30). In this work, the use of fluorescently labeled germination proteins revealed that the germinosome has a different appearance in dormant and germinated spores, discrete foci in dormant spores that become dispersed as spore germination proceeds. Levels of GR subunits and SpoVA proteins remained relatively unchanged after 2 hr of germination, although upon germinated spore outgrowth and conversion into vegetative cells at an OD_{600} of 2, the majority of these proteins' levels had decreased more than 50%.

In contrast to GR subunits and SpoVA proteins, GerD levels decreased ≥ 50% as early as 15 min post germinant addition. This decrease in GerD level was observed not only in germinating wild-type spores, but also in germinating *gerD-gfp* and *gerAA-mCherry* spores, indicating that the fusion proteins did not alter the behavior of endogenous GerD. We also tested the stability of GerD-GFP by western blot analysis of extracts of dormant and germinating KGB09 (*ΔgerD amyE::gerD-gfp*) spores that lack endogenous GerD and found that <5% of the fusion protein appeared at the position of native GerD (data not shown). The decrease in total spore GerD level early in spore germination is consistent with previous reports of decreases in GerD levels in isolated IM from germinated spores (9,66). In addition, levels of native GerD fell essentially to zero as germinated spores outgrew and became vegetative cells. Since germinosome formation in dormant spores requires GerD (30), it is not unreasonable that germinosome dispersion

in germination might be due at least in part to decreased levels of GerD. This loss of GerD soon after initiation of germination is presumably due to proteolysis, and GerD becomes sensitive to both an externally added protease and a biotinylation agent in germinated spores, while is resistant to this protease and biotinylation agent in dormant spores, even decoated dormant spores (42). Perhaps in dormant spores GerD is shielded from protease digestion and biotinylation in the germinosome foci, and become accessible to these treatments when the germinosome disperses. The sensitivity of GerD to a protease and an external biotinylation agent in germinated spores suggests that GerD is on the outer surface of the germinated spore's IM, and presumably in dormant spores as well. This location of GerD-GFP is, however, somewhat at odds with the fact that GFP generally does not fold properly after crossing a membrane, especially the plasma membrane of Gram negative bacteria, as most proteins fused to GFP that are secreted into the periplasm do not exhibit significant fluorescence (13). However, unlike the periplasm of Gram negative bacteria that is an oxidizing environment (13), the space between the developing spore's IM and outer membrane is not in direct contact with the sporulation medium, and could well be a reducing environment, just as in the forespore cytoplasm. Unfortunately, there are no data on the precise conditions in this compartment of sporulating cells.

GerD is a helical trimer *in vitro*, and may be capable of forming even higher order oligomeric structures (47). In addition, GerD-GFP can form germinosome-like foci in dormant spores even in the absence of GRs (30). These results suggest that GerD may self-associate to form a scaffold on which the GRs bind to form the germinosome, and perhaps this scaffold can facilitate signal transmission events in germination. However,

when this GerD scaffold protein is lost, the germinosome can no longer maintain its structural integrity and disperses. Unfortunately, *in vitro* affinity pull-down experiments with purified GerD indicate that GerD does not associate with at least GerBC (45,46). Possible explanations for this negative result could be that GerD and GR proteins interact exclusively when both are on membrane, or that GerD interaction with GRs in the germinosome is not through GRs' C subunits.

The demonstration that a *cwlD* mutation prevents germinosome dispersion in spore germination indicates that germinosome dispersion requires at least progression through stage II of germination, and this is consistent with the kinetics of germinosome dispersion during spore germination. The rapid > 50% decrease in the GerD level ~ 15 min into spore germination suggests that the germinosome might disperse early in germination, even though levels of most other known germinosome constituents remained relatively normal for up to two hr. However, germinosome dispersion during germination was clearly significantly slower than the loss of > 50% of GerD in the first 15 min of germination, taking place 15-30 min after completion of spore germination. Why might germinosome dispersion be so much later than a significant drop in the GerD level? An obvious answer to this question is that the > 2-fold decrease in GerD level early in germination alone is insufficient to cause immediate germinosome dispersion. In addition, perhaps the GerD rapidly degraded early in germination is not interacting with GRs. If the latter is the case, GerD might be more stable in spores with higher GR levels, and more rapidly and completely degraded early in the germination of spores with low GR levels. However, this was not the case, as spores of strains PS3476 overexpressing the GerA GR ~ 8-fold (28), PS3665 containing only the GerB* GR that has a single

amino acid change allowing spore germination with L-asparagine alone (5), and PS533 (wild-type) (81) lost GerD at essentially identical rates during spore germination (data not shown). Since average numbers of GR molecules in spores of the latter 3 strains are ~ 10,000 (PS3476), 2,500 (PS533) and 700 (PS3665) (92,93), it appears clear that the numbers of GR subunits available for interaction do not influence GerD stability during spore germination.

Another piece of evidence suggesting that loss of GerD is not the crucial event leading to germinosome dispersion in spore germination is that germinosome dispersion took place not only in spores with an mCherry fusion to GerAA or GerKB, but also in spores with a GFP fused to GerD, yet we found that GFP-GerD is stable throughout spore germination. Since GFP-GerD is functional in spore germination (30), either a germinosome with GFP-GerD is inherently much less stable than a germinosome with wild-type GerD, or some factor or factors other than GerD levels is crucial for germinosome stability. What might this other factor or factors be? While we cannot yet answer this question definitively, we know that the dormant *B. subtilis* spore IM environment is very different from that in a growing cell or a germinated spore. As noted in the introduction, the mobile fraction of IM lipids rapidly increases ~ 2.5-fold early after completion of stage II of *B. subtilis* spore germination, and to a value essentially identical to that of the mobile fraction in vegetative cells' plasma membrane (12). However, even with this change, the diffusion coefficient of mobile germinated spore IM lipid only increases ~ 2-fold over that in dormant spores IM, and is still ~ 9-fold lower than in the vegetative cell plasma membrane (12). Perhaps it is a change in the germinated spore's IM resulting in a further increase in the lipid diffusion coefficient in

the IM to a value closer to that in the vegetative cell plasma membrane that results in germinosome dispersion. However, when this latter change in lipid diffusion coefficient takes place during spore germination is not known.

The kinetics of the germinosome dispersion process might also be affected by the strength of the interactions that hold proteins together in the germinosome, a structure that may exist in a transient interacting state, since the signal facilitated by the germinosome that triggers CaDPA release from the spore core occurs in a very short time period, and well before the germinosome disperses after completion of spore cortex hydrolysis. Transient protein interactions, or the "soft wired signaling concept" suggests that signaling proteins translocate and have reversible binding interactions as part of their overall signaling pathway (63,101). In *B. subtilis* spores the protein-protein interactions in the germinosome, in particular between the GRs and GerD and between GRs and GRs, could be promoted by changes in the IM during sporulation. As the IM is compressed when dormant spores are formed, the amount of germination proteins present brings GerD trimers into close proximity with both other GerD trimers and with GRs, promoting germinosome formation through multiple weak protein-protein interactions, and these interactions become fixed because of the minimal mobility of lipids in the dormant spore IM. As the IM expands after T_{lys} and lipid mobility increases, GerD becomes accessible to proteases and is degraded, while the GRs slowly diffuse away through the milieu of the now largely mobile IM. It is also possible that GRs exist in two different conformations, one receptive to interacting with other GRs and GerD in dormant spores, and one in germinated spores when the GRs change conformation and are no longer receptive to interaction with GerD. No direct evidence exists for this possibility, however there is

evidence for membrane proteins existing in two conformations (95,96). It is clear that further experimentation is required to understand germinosome dynamics, and analysis of the kinetics of and factors required for germinosome formation during sporulation may give particularly valuable information; this work is currently in progress.

ACKNOWLEDGEMENTS

We thank Keren Griffiths for creating strains KGB09, KGB72 and KGB94. This work was supported by a Department of Defense Multi-disciplinary University Research Initiative through the U.S. Army Research Laboratory and the U.S. Army Research Office under contract number W911F-09-1-0286 (PS/JY/AC), and by a grant from the Army Research Office under contract number W911NF-12-1-0325.

Table 3-1. *B. subtilis* strains used*

Strain	Genotype and phenotype	Source (reference)
PS533	wild-type pUB110 Km^r	(81)
PS2307	PS832 Δ*cwlD* Cm^r	(74)
PS3476	PS832 P*sspD*::*gerA* MLS^r	(28)
PS3665	FB10 Δ*gerA gerB* ΔgerK* MLS^r Sp^r	(5)
PS4150	PS832 Δ*gerE* Δ*cotE* Sp^r Tc^r	(2)
KGB09	PS832 Δ*gerD amyE::gerD-gfp* Cm^r Sp^r	Keren Griffiths
KGB72	PS4150 *gerKB-mCherry* Cm^r	(30)
KGB73	PS4150 *gerD-gfp* Km^r	(30)
KGB80	PS4150 *gerKB-mCherry gerD-gfp* Cm^r Km^r	(30)
KGB94	PS4150 *gerD-gfp* Δ*cwlD* Cm^r Km^r	This study
KGB114	PS4150 *amyE::gerAA-mCherry* Cm^r	(30)

*Abbreviations used are resistance to: Cm^r, chloramphenicol (10 μg/ml); Km^r, kanamycin (10 μg/ml); MLS^r, erythromycin (1 μg/ml) and lincomycin (25 μg/ml); Sp^r, spectinomycin (100 μg/ml); and Tc^r, tetracycline (10 μg/ml).

Table 3-2. Germinosome appearance in dormant and germinating *cwlD* spores*

	No. (%) of spores		
		At germination time of:	
Germinosome appearance	Dormant	1 h	2 h
Foci	157 (95)	120 (90)	135 (89)
Disperse	2 (1)	3 (2)	3 (2)
No signal	6 (4)	11 (8)	14 (9)

*Fluorescence and DIC images of KGB94 (PS4150 *gerD-gfp* Δ*cwlD*) spore populations were analyzed in dormant spores and after 1 and 2 hr of germination as described in Methods, and germinosome appearance in individual spores was scored as foci or disperse as seen in Fig. 3-4.

Table 3-3. Germinosome appearance in dormant spores, and during spore germination*

Germinosome appearance	No. (%) of spores				
		Spores at germination time (min) (% germination) of[b]:			
	Dormant	15 (10)	30 (50)	60 (70)	120 (80)
Foci	203 (91)	178 (89)	180 (81)	25 (12)	28 (12)
Disperse	17 (8)	19 (10)	37 (17)	157 (76)	161 (67)
No signal	4 (2)	4 (2)	5 (2)	24 (12)	51 (21)

*Quantitation of spore germination and germinosome appearance in dormant KGB72 (PS4150 *gerKB-mCherry*) spores, and germinated (low refractive index) KGB72 (30, 60 and 120 min samples) spores or KGB72 and KGB80 (PS4150 *gerKB-mCherry gerD-gfp*) (15 min sample) spores germinated in glass bottom dishes as described in Methods. Numbers for 15 min samples are from both KGB72 and KGB80 spores to ensure obtaining sufficient numbers of spores that germinated at this time point; germinated spores of both strains gave essentially identical results. Fluorescence images were analyzed in dormant spores and after various germination times, and germinosome appearance in individual spores was scored as described in the legend to Table 2.

[b]The percentage of spore germination was determined by examining the DIC image intensity of > 500 individual spores at each time point. Values shown are for KGB72 spores, and values for KGB80 spores were essentially identical.

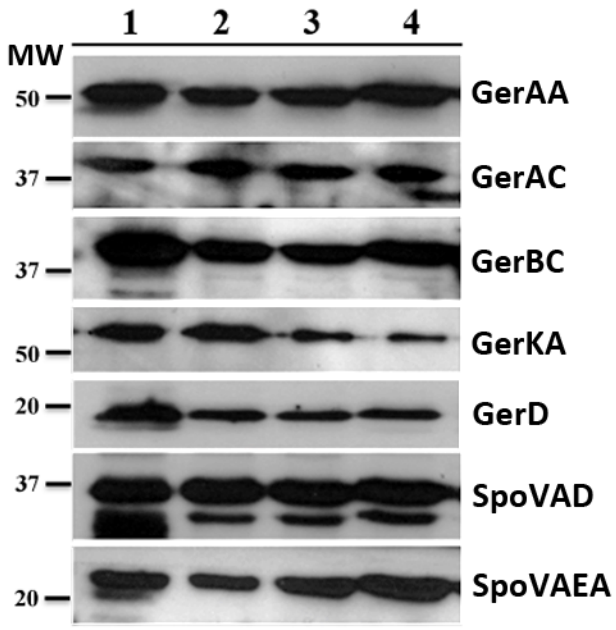

Fig. 3-1. Western blot analysis of germination protein levels in the L fraction of dormant and germinating PS4150 spores. The L fraction from spores was isolated, equal amounts of protein run on SDS-PAGE and western blots were probed with various antisera. Spore samples run in various lanes are: 1 – dormant; 2 – 15 min germination; 3 – 60 min germination; 4 – 120 min germination; MW – molecular weight markers in kDa. The band running just below SpoVAD is likely a breakdown product of this protein that has been seen previously (6,7).

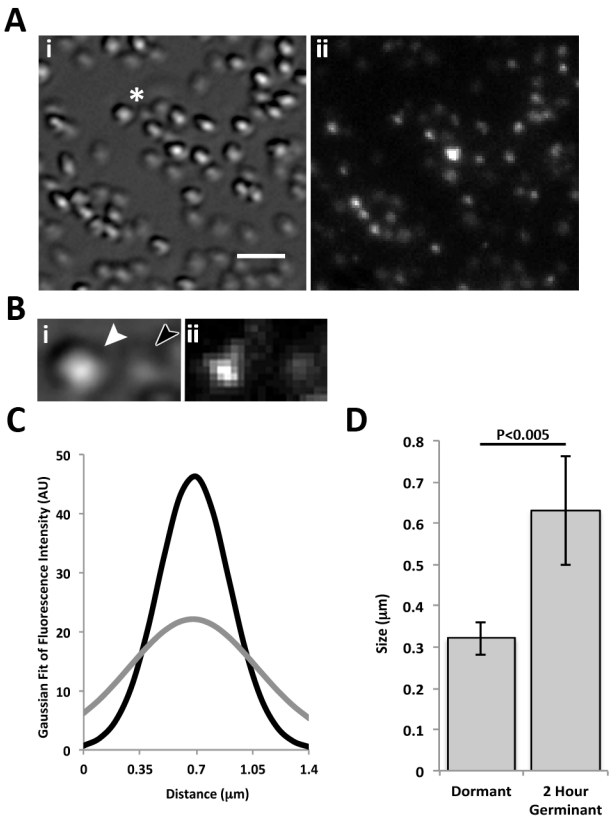

Fig. 3-2A-D. DIC and fluorescence microscopic analysis of germinating KGB73 (PS4150 *gerD-gfp*) spores. A) DIC (i) and fluorescence (ii) images of spore populations 2 hr post-germinant addition as described in Methods. The scale bar in (i) is 2 μm and (i) and (ii) are at the same magnification. (B) 2.5x magnification of area marked by white asterisk in panel (A); DIC image (i) showing a dormant (white arrow) and a germinated (dark arrow) spore and (ii) fluorescence image. (C) Average Gaussian fit of background-subtracted fluorescence intensity along the long axis of 20 dormant spores (black curve) and the same spores after 2 hr of germination (grey curve). All germinated spores had T_{lys} times that were < 1 hr. (D) Graph of change in (σ) of Gaussian distributions from (C) in dormant and 2 hr germinating spores. Error bars represent one standard deviation, and the P-value for the difference between dormant and germinated spores is given above the graph.

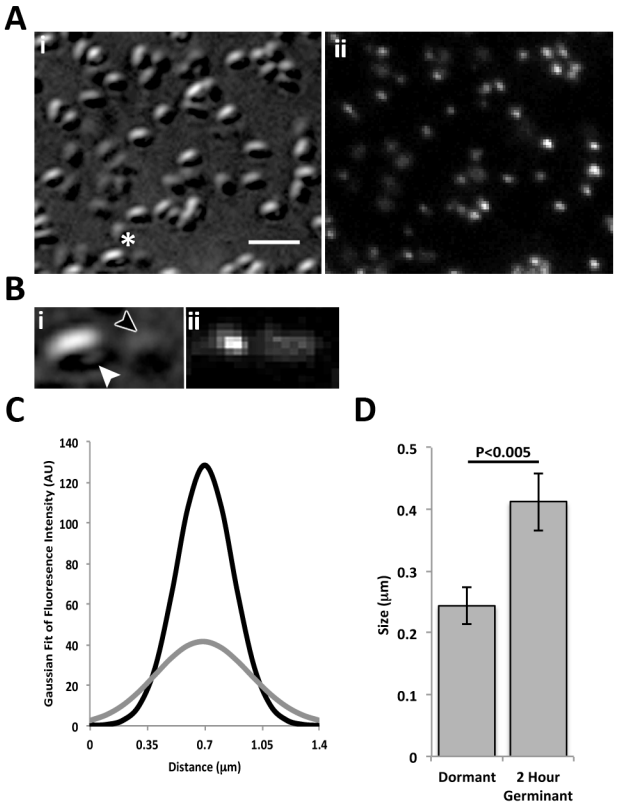

Fig. 3-3A-D. DIC and fluorescence microscopic analysis of germinating KGB114 (PS4150 *gerAA-mCherry*) spores. A) DIC (i) and fluorescence (ii) images of spore populations 2 hr post germinant addition. The scale bar in (i) is 2 μm and the magnifications in (i) and (ii) are identical. (B) 2.5x magnification of area marked by white asterisk in panel (A); DIC image (i) showing a dormant (white arrow) and a germinated (dark arrow) spore and fluorescence image (ii). (C) Average Gaussian fit of fluorescence intensity along the long axis of 20 dormant (black curve) spores and the same 20 spores after 2-hr of germination (grey curve). All spores had T_{lys} times of < 1 hr. (D) Graph of change in (σ) of Gaussian distributions from (C) in dormant and 2 hr germinating spores. Error bars represent one standard deviation and P-value is given above the graph.

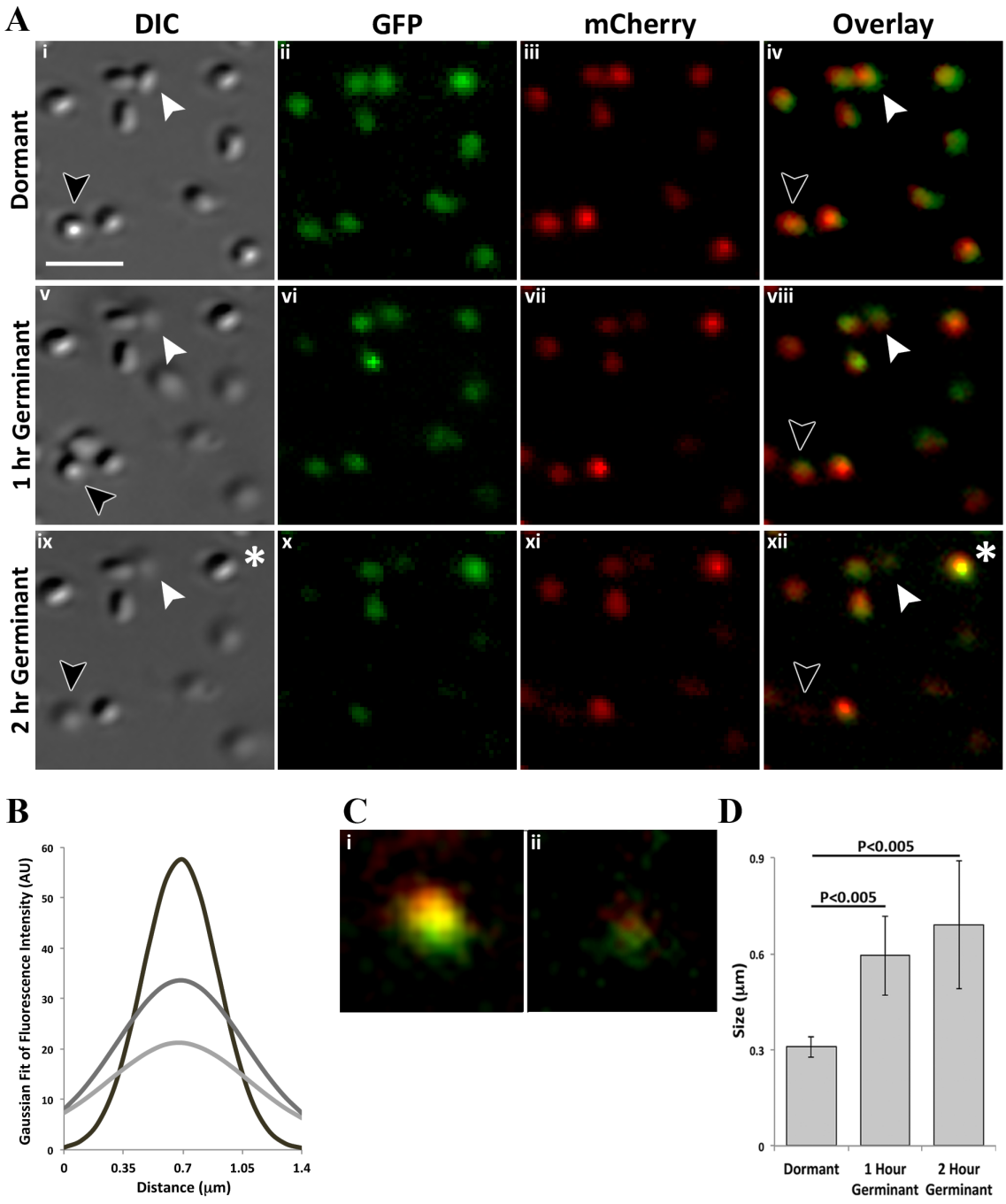

Fig. 3-4A-D. Time-lapse microscopy of germinating double fluorescent fusion (PS4150 *gerKB-mCherry gerD-gfp*) spores. (A) DIC images (i, v, ix), fluorescence images of GFP (ii, xi, x), mCherry (iii, vii, xi) or GFP/mCherry overlay (iv, viii, xii). The field of view was kept stationary to track the same spores throughout the experiment.

The scale bar in panel (Ai) is 2 μm, and panels (i-xii) are at the same magnification. White arrows indicate spores with T_{lys} times that were < 1 hr and black arrows indicate spores with T_{lys} times that were > 1hr. The asterisk in (Axii) indicates a dormant spore at 2 hr post-germinant addition, with no photobleaching apparent over the 2 hr experiment. (B) Gaussian fit of overlay fluorescence intensity along the long axis of 30 dormant spores (black curve), and the same 30 spores at 1 or 2 hr post-germinant addition that had germinated before 1 hr (dark grey, and light grey curves, respectively). (C) 3.5X magnification of spores from 2-hr germination fluorescence overlay panel (Axii). We define germinosome phenotype as a discrete focus (Ci) or a dispersed signal (Cii). Dormant spore (i) (Axii, asterisk), and germinated spore (ii) with a < 1 hour (Axii, black arrow). (D) Graph of change in (σ) of Gaussian distributions from (B). Error bars represent one standard deviation, and P-values are shown above the graph.

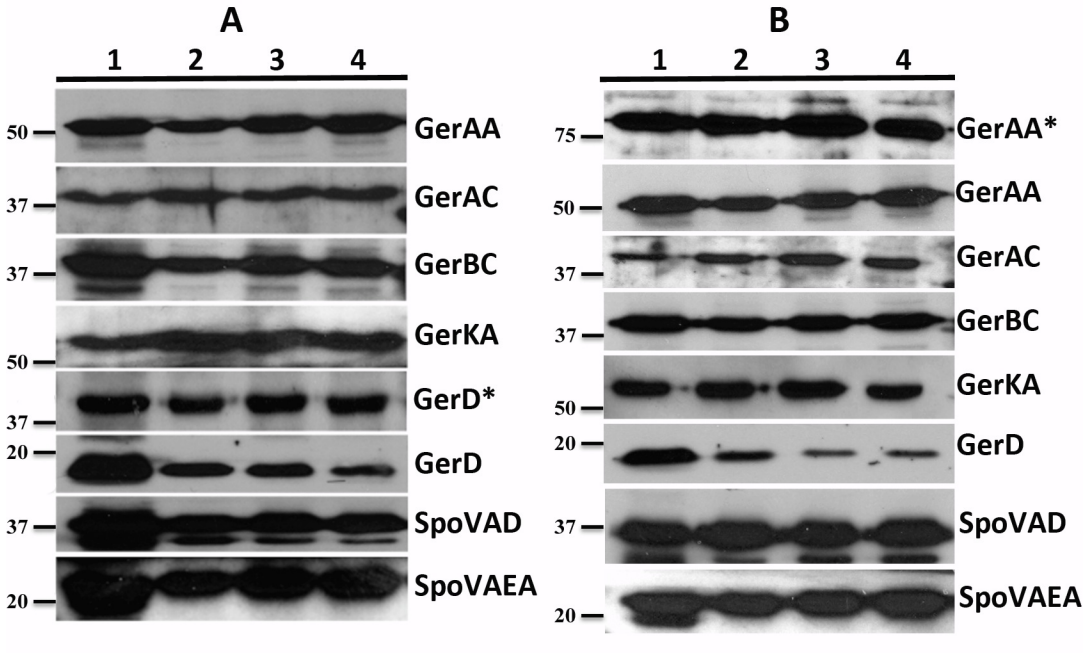

Fig. 3-5A,B. Western blot analysis of germination protein levels in spores of strains KGB73 (PS4150 *gerD-gfp*) (A) and KGB114 (PS4150 *gerAA-mCherrry*) (B). The L fraction of dormant and germinating spores was isolated, equal amounts of protein run on SDS-PAGE, and subjected to western blot analysis with various antisera. Spore L fractions run on lanes in both panels are: 1 – dormant; 2 – 15 min germination; 3 – 60 min germination; and 4 – 120 min germination. The migration positions of molecular weight markers in kDa are shown to the left of the panels. Proteins labeled with asterisks indicate a fluorescent fusion protein that ran at higher mol wt than the native protein.

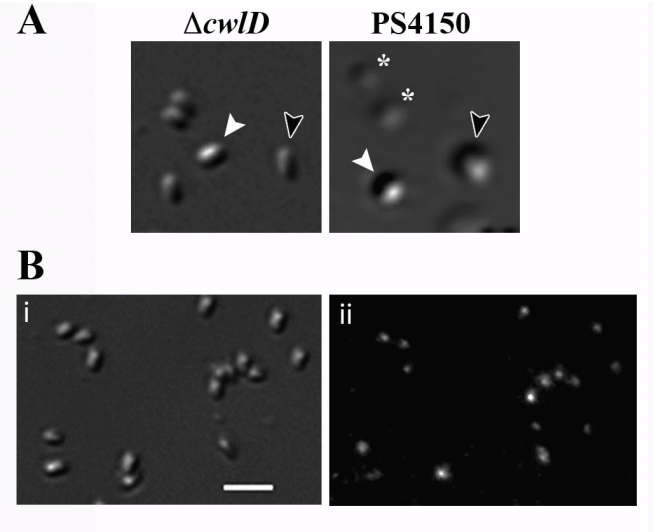

Fig. 3-6A,B. Differential interference contrast microscopy of spores after 2 hr of germination. (A) KGB94 (PS4150 *gerD-gfp* Δ*cwlD*) (Δ*cwlD* panel) and PS4150 spores were germinated for 2 hr at 37°C in glass bottom dishes as described in Methods, and imaged by DIC microscopy. White arrows indicate a dormant spore (high refractive index), black arrows indicate a germinating spore after completion of CaDPA release (low refractive index), and asterisks indicate germinating spores after the completion of cortex hydrolysis (lowest refractive index). (B) KGB94 spores were germinated for 2hr at 37°C in glass bottom dishes as in (A) and imaged by DIC (i) and epifluorescence (ii) microscopy. Scale bar in panel (i) is two microns.

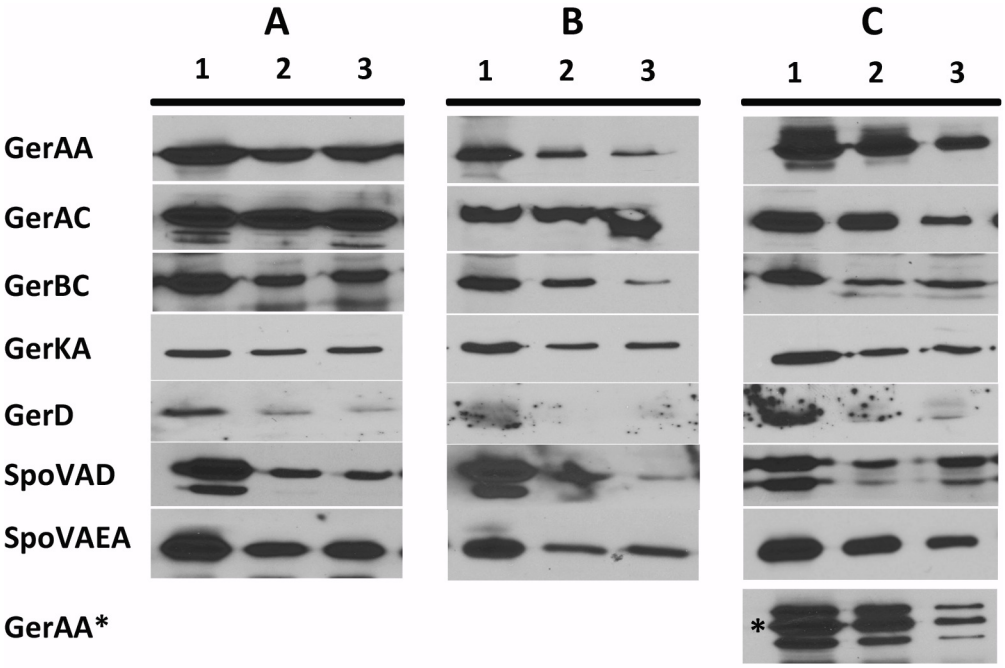

Fig. 3-7A-C. Western blot analysis of germination protein levels in germinated and outgrowing spores of strains (A) PS4150 (wild-type), (B) KGB73 (PS4150 *gerD-gfp*) and (C) KGB114 (PS4150 *gerAA-mCherrry*). The L fractions of equal volumes of 2 hr germinated as well as outgrowing spores were isolated, and equal volumes of sample run on SDS-PAGE, and subjected to western blot analysis with various antisera. Spore lysates run on lanes in all panels are: 1 – 2 hour germination; 2 – outgrown to OD_{600} = 1; and 3 – outgrown to OD_{600} = 2. All proteins ran at the expected molecular weight. Proteins labeled with asterisks indicate a fusion protein that ran at higher molecular weight than the normal protein.

CHAPTER 4

SUMMARY OF WORK AND FUTURE DIRECTIONS

4-1 The Lifecycle of the Germinosome

Previous work showed that the GRs and GerD colocalize in a single focus in dormant spores in a GerD dependent manner (30). From our current work, we have analyzed the germinosome in the context of sporulation, germination, and outgrowth, revealing how the complex is formed, maintained, and ultimately disperses. Not surprisingly, we found that in sporulation, the germinosome forms in a GerD dependent manner, and it does so nearly in parallel with GerD synthesis after engulfment of the developing forespore. Germinosome formation occurred ~3 hours before DPA uptake into spores, as well as before spore maturation in stage VI of sporulation when the IM compresses and the lipids within it become immobile. GerD was also found to form foci independently of the GRs and independently of its environment, showing it has the ability to self-associate, and suggesting that it forms a scaffold for the GRs to localize to. Moreover, the IM was not a significant factor in facilitating germinosome formation, in contrast to an earlier suggestion that the compression of the inner membrane may force germinosome constituents into close proximity, and loss of IM lipid mobility "freezes" the protein complex in place. While not essential for germinosome formation, the IM perhaps contributes to germinosome stability after it has formed.

Once the germinosome is formed, it remains that way up through stage I of germination (103). Levels of GR subunits and SpoVA proteins, the latter of which are not associated with the germinosome (30), remain relatively unchanged after 2 hr of germination, and do not begin to decrease until well into outgrowth (103). However, in contrast to the GR subunits and SpoVA proteins, GerD levels decreased ≥ 50% as early as 15 min post germinant addition (103). This was counterintuitive to our hypothesis that

GerD was critical in forming and specifically maintaining the germinosome. Our results clearly indicated that the dispersion of the germinosome took place 15-30 min after completion of spore germination, significantly slower than GerD levels decreasing > 50% in the first 15 min of germination. Therefore, we believe that the >2-fold loss of GerD by itself in not enough to cause immediate germinosome dispersion, and other factors are involved. One other possible factor is that the mobility of the lipids in the IM may effect the stability of the germinosome; the mobile fraction of IM lipids rapidly increases ~2.5 fold after stage II of *B. subtilis* spore germination, whereas the diffusion coefficient only increased ~2-fold over that in dormant spores. However, this diffusion coefficient is still ~9-fold lower than that of the vegetative cell plasma membrane. This large change in the spore's IM could affect germinosome dispersion. What is clear from our work is that the germinosome, while dependent on GerD for its formation, is not as dependent on GerD to remain colocalized after spore germination begins.

4-2 A Model for Signal Transduction

In *Bacillus subtilis* spore germination, GerD is essential in the formation of the germinosome. When GerD is deleted, the GRs fail to colocalize in discrete foci, and rates of nutrient germination diminish significantly (30,65). However, soon after spore germination begins, levels of GerD protein decrease significantly while the germinosome remains intact, indicating that once nutrient germination is initiated, normal GerD levels are no longer essential for germinosome stability. It is possible that whatever signal is facilitated by GerD and the germinosome that is transduced quickly to downstream effectors, is only required for a "snapshot" in time. Therefore, once germination is

initiated, and the nutrient signal from the environment has travelled via the germinosome to downstream effectors, GerD is no longer required and begins to be degraded within 15 min of germinant addition.

Therefore, we propose a germinosome model where GerD exists as a "snapshot" protein: 1) in sporulating *B. subtilis*, immediately after protein synthesis, GerD self associates and forms the germinosome scaffold to which the GRs bind; 2) the colocalized proteins remain fixed in place as the developing forespore IM matures into largely immobile dormant spore IM; 3) upon receiving a nutrient signal from the environment this signal is transduced via the germinosome to downstream effectors and spore germination begins; 4) early in germination levels of GerD begin to decrease, the spore IM expands ~2 fold, and spore IM lipid mobility is restored, all of which facilitate the dispersion of the germinosome. In this model, GerD functions to create a scaffold for the germinosome to form, and to transduce whatever signal triggers CaDPA release from the spore core. This occurs in a very short time period, and as a result GerD is only required for a snapshot in time, before this protein ultimately becomes degraded in germinating spores (103).

4-3 Future Directions

The studies presented in this dissertation are of importance to the field of spore germination as the results give a better understanding of how a cluster of spore germination proteins, the germinosome, functions in nutrient spore germination. Specifically, what the function of GerD is in the multiprotein complex, and how it functions in the signal transduction process of spore nutrient germination. However,

many questions remain regarding the germinosome, specifically in the protein-protein interactions within the complex, and how the complex is structurally organized.

Bacillus subtilis spores are incredibly small, ~1000 nm in length and ~500 nm in width, which presents a distinct challenge when doing microscopy studies. The maximum axial resolution for conventional confocal microscopy is ~1 μm, which is larger than the width of a *B. subtilis* species spore. Using a modified epifluorescence microscope (IX81 Olympus, Center Valley, PA, USA) with a TE-cooled EM-CCD camera (Princeton Instruments, Trenton, NJ, USA), the depth-of-the-field is ~700, which allowed us to take images reflecting the fluorescence signal from the entire spore, including the top and bottom surfaces. However, the foci observed in our experiments appear as diffraction-limited spots, as on average their fluorescence signal fit a Gaussian function with full width at half maximal intensity of ~300 nm (30,103), which is the optical resolution of the microscope used. Super-resolution microscopy methods would allow for better observation of the germinosome, and possibly give insight into the structural organization of this multiprotein complex.

Photoactivated localization microscopy (PALM) has been performed on the germinosome, and it was found the complex is closer to ~100 nm in size, well below the resolution of our epifluorescence microscope (unpublished data). If PALM was attempted using different fluorophores for different germination proteins, perhaps a better understanding of the spatial organization of the germinosome could be elucidated. Furthermore, vertico spatially modulated illumination (VSMI) has been shown to reach resolutions as small as 40 nm in 3D analyses (78). VSMI is a combination of spectral precision distance microscopy (SPDM) and spatially modulated illumination (SMI). First

the SMI process determines the center of particles and their spread in the direction of the microscope axis, then SPDM determines the lateral position of the individual particles. Using this method a 3D color reconstruction of the spatial arrangements of Her/neu and Her3 clusters in all three directions could be determined with an accuracy of ~25 nm (39). If this technology could be applied to our studies of the germinosome, perhaps we could better determine how the germinosome is organized and obtain clues to the protein-protein interactions within it.

Another poorly understood facet of *B. subtilis* spore germination is the structure of the spore IM. It is know the IM lipids exist in a relatively immobile and compressed state in dormant spores, and upon germination this lipid mobility is restored and the IM volume expands ~1.5 to ~2-fold, all of which occurs without any new membrane synthesis or ATP production. As a result, we believe the structure of the spore IM may have some novel feature to it, possibly a unique way it folds on itself, which could facilitate protein-protein interactions within it. However, attempting to isolate the spore IM by removing the spore coat and cortex removes the native environment the dormant spore IM resides in, and thus the isolated IM is not an accurate representation of the dormant spore IM. One possible technique that may be able to give insight into the dormant spore IM is cryo-electron microscopy (cryo-EM). This process allows for imaging of specimens in their native environments, and recently has shown structures of viruses, mitochondria, ribosomes, ion channels, and enzyme complexes at near atomic resolution (4.5 Å) (43). The benefit of using cryo-EM to study the structure of the germinosome is that the molecule of interest does not have to be manipulated heavily, as it is for X-ray crystallography, and instead a thin film of an aqueous solution is rapidly

frozen on a support grid (so fast that water has no time to crystallize). This thin film is placed in the vacuum of the electron microscope, where it is cooled with liquid nitrogen to -180^{o}C, and projection images of multiple copies of the molecule suspended in random orientations are recorded with a 200 kV or 300 kV beam of electrons. The spore inner membrane contains large volume of proteins, therefore any type of electron microscopy would be a challenging endeavor, but perhaps cyro-EM could yield some clues as to the novel environment of the inner spore membrane and how it effects the germinosome.

Lastly, as mentioned previously the crystal structure of the core domain of GerD has been solved, which displayed a novel protein that exists as a superhelical trimer capable of self-associating into higher order structures (47). However, the only other crystal structure of a germinosome protein that has been solved is GerBC, which was found not to interact with GerD (46). Although GerAC does somehow interact with GerD in E. coli (Fig. 2-5), perhaps the interaction is different when in the milieu of the spore inner membrane. Currently, our understanding of protein-protein interactions among the GRs and GerD is limited; it has been shown by crosslinking studies on isolated IM *in vitro* that GerAA interacts with itself and GerD interacts with itself (92). However, crosslinking studies were unable to identify any protein-protein interactions in dormant spores, possibly due to permeability barriers presented by the structure of the spore. If the crystal structures of other germinosome protein subunits are solved in the future, we may be able to create a 3-dimensional model for how the complex is organized. Specifically if the interactions among proteins in the germinosome are transient, solving the crystal structures of the proteins may show us how these transient interactions occur.

APPENDIX A

UNPUBLISHED DATA

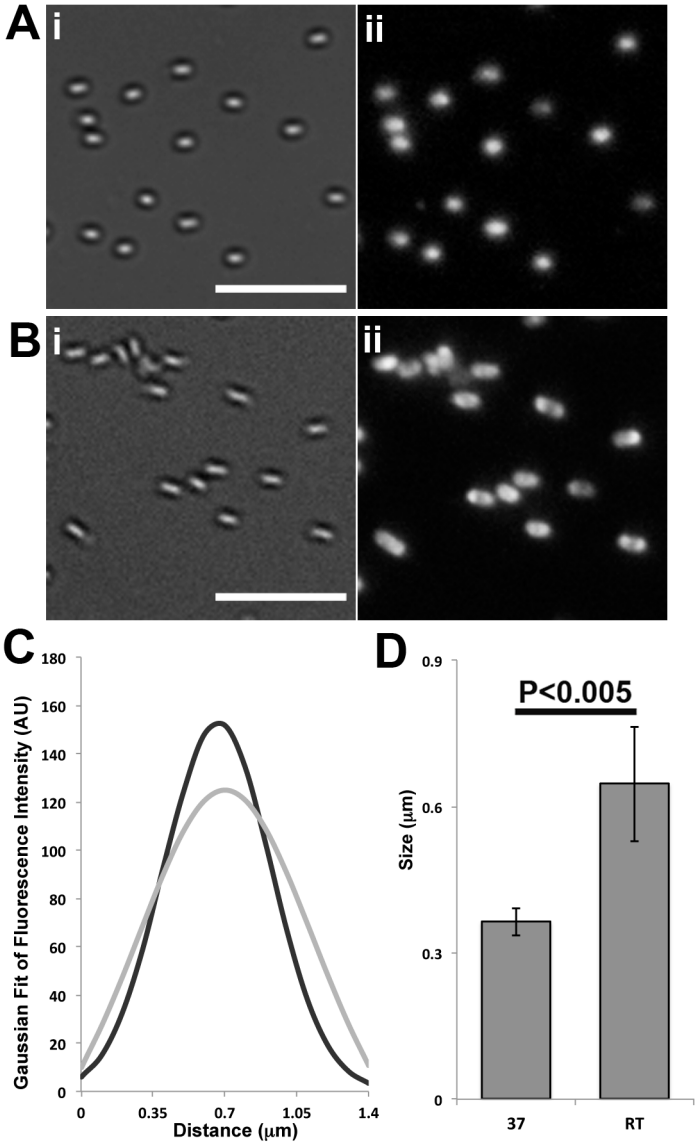

Fig. 5-1A-D. DIC and fluorescence microscopic analysis of KGB73 (PS4150 *gerD-gfp*) spores at different sporulation temperatures. A) DIC (i) and fluorescence (ii) images of spore populations sporulated at 37°C. The scale bar in (i) is 5 μm and (i) and (ii) are at the same magnification. (B) DIC (i) and fluorescence (ii) images of spore populations sporulated at room temperature (RT), ~23°C. The scale bar in (i) is 5 μm and (i) and (ii) are at the same magnification. (C) Average Gaussian fit of fluorescence

intensity along the long axis of 20 spores sporulated at 37^{o}C (black curve) and 20 spore sporulated at RT (grey curve). (D) Graph of (σ) of Gaussian distribution from (C) in KGB73 sporulated at 37^{o}C and KGB73 sporulated at RT. Error bars represent one standard deviation and P-values determined by students two-tailed T-test are given above the graph.

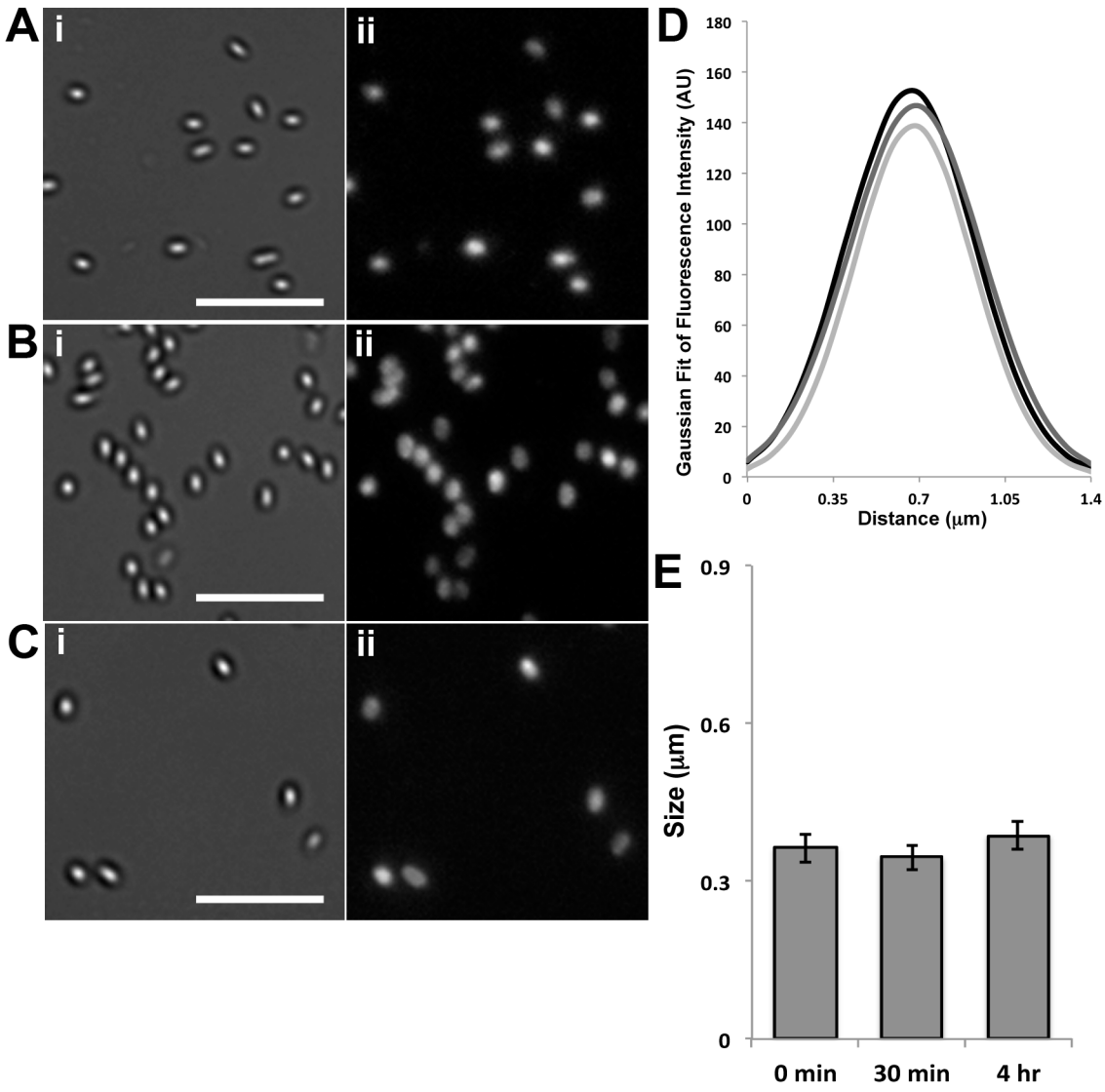

Fig. 5-2A-E DIC and fluorescence microscopic analysis of KGB73 (PS4150 *gerD-gfp*) spores after heat activation. Previous work showed that varying heat activation duration at 75°C on *B. subtilis* spores resulted in increased rates of spore germination (49). However, we found that varying duration of heat activation on *B. subtilis* spores had no effect on the germinosome. A) DIC (i) and fluorescence (ii) images of spore populations without heat shock. The scale bar in (i) is 5 μm and (i) and (ii) are at the same magnification. (B) DIC (i) and fluorescence (ii) images of spore populations heat

shocked at 75°C for 30 min. The scale bar in (i) is 5 μm and (i) and (ii) are at the same magnification. (C) DIC (i) and fluorescence (ii) images of spore populations heat shocked at 75°C for 4 hr. The scale bar in (i) is 5 μm and (i) and (ii) are at the same magnification. (D) Average Gaussian fit of fluorescence intensity along the long axis of 20 spores with no heat shock (black curve), 20 spores heat shocked at 75°C for 30 min (dark grey curve), and 20 spores heat shocked at 75°C for 4 hr (light grey curve). (E) Graph of (σ) of Gaussian distribution from (D) in KGB73 heat shocked at 75°C for 0 min, 30 min, and 4 hr. Error bars represent one standard deviation and students two-tailed T-test determined the data was not statistically significant.

REFERENCES

1. **Abanes-De Mello A, Sun YL, Aung S, Pogliano K**. 2002. A cytoskeleton-like role for the bacterial cell wall during engulfment of the *Bacillus subtilis* forespore. Genes Dev. **16**:3253-3264.

2. **Atluri S, Ragkousi K, Cortezzo DE, Setlow P**. 2006. Cooperativity between different nutrient receptors in germination of spores of *Bacillus subtilis* and reduction of this cooperativity by alterations in the GerB receptor. J Bacteriol. **188**:28 –36.

3. **Ball DA, Taylor R, Todd SJ, Redmond C, Couture-Tosi E, Sylvestre P, Moir A, Bullough PA**. 2008. Structure of the exosporium and sub layers of spores of the *Bacillus cereus* family revealed by electron crystallography. Mol Microbiol. **68**:947-958.

4. **Butzin XY, Troiano AJ, Coleman WH, Griffiths KK, Doona CJ, Feeherry FE, Wang G, Li YQ, Setlow P**. 2012. Analysis of the effects of a gerP mutation on the germination of spores of *Bacillus subtilis*. J Bacteriol. **21**:5749-5758.

5. **Cabrera-Martinez RM, Tovar-Rojo F, Vepachedu VR, Setlow P.** 2003. Effects of overexpression of nutrient receptors on germination of spores of *Bacillus subtilis* J Bacteriol. **185:**2457-2464.

6. **Camp AH, Losick R**. 2009. A feeding tube model for activation of a cell-specific transcription factor during sporulation in *Bacillus subtilis*. Genes Dev. **23**:1014-1024.

7. **Chary VK, Meloni M, Hilbert DW, Piggot PJ**. 2005. Control of the expression and compartmentalization of σ^G activity during sporulation of *Bacillus subtilis* by regulators of σ^F and σ^E. J Bacteriol **187**:6832-6840.

8. **Chary VK, Xenopoulos P, Piggot PJ**. 2006. Blocking chromosome translocation during sporulation of *Bacillus subtilis* can result in prespore-specific activation of σ^G that is independent of σ^E and of engulfment. J Bacteriol **188**:7267-7273.

9. **Chen Y, Ray WK, Helm RF, Melville SB, Popham DL.** 2014. Levels of germination proteins in *Bacillus subtilis* dormant, superdormant and germinating spores. PLoS One **9**:e95781.

10. **Christie G, Gotzke H, Lowe CR**. 2010. Identification of a receptor subunit and putative ligand-binding residues involved in the *Bacillus megaterium* QM B1551 spore germination response to glucose. J Bacteriol. **192**:4317–4326.

11. **Cowan AE, Koppel DE, Setlow B, Setlow P**. 2003. A soluble protein is immobile in dormant spores of *Bacillus subtilis* but is mobile in germinated spores: implications for spore dormancy. Proc Natl Acad Sci. U. S. A. **100**:4209 – 4214.

12. **Cowan AE, Olivastro EM, Koppel DE, Loshon CA, Setlow B, Setlow P.** 2004. Lipids in the inner membrane of dormant spores of *Bacillus* species are largely immobile. Proc Natl Acad Sci USA. **101:**7733–7738.

13. **Dammeyer T, Tinnefold P.** 2012. Engineered fluorescent proteins illuminate the bacterial periplasm. Comp Struct Biotechnol. **3**:e201210013.

14. **de Hoon M JL, Eichenberger P, Vitkup D**. 2010. Hierarchical evolution of the bacterial sporulation network. Curr Biol. **20**:735-745.

15. **de Jong IG, Beilharz K, Kuipers OP, Veening JW**. 2011. Live cell imaging of *Bacillus subtilis* and *Streptococcus pneumoniae* using automated time-lapse microscopy. J Vis Exp. **53**: 3145.

16. **Doan T, Morlot C, Meisner J, Serrano M, Henriques A, Moran C, Rudner DZ**. 2009. Novel secretion apparatus maintains spore integrity and developmental gene expression in *Bacillus subtilis*. PLoS Genet. **5**:e1000566.

17. **Driks A**. 1999. Bacillus subtilis spore coat. Microbiol Mol Biol Rev. **63**:1–20.

18. **Duncan L, Alper S, Arigoni F, Losick R, Stragier P**. 2005. Activation of cell-specific transcription by a serine phosphatase at the site of asymmetric division. Science. **270**:641-644.

19. **Eichenberger P, Fujita M, Jensen S, Conlon E, Rudner D, Wang S, Ferguson C, Haga K, Sato T, Liu JS, Losick R**. 2004. The program of gene transcription for a single differentiating cell type during sporulation in *Bacillus subtilis*. PLoS Biol. **2**:e328.

20. **Eswaramoorthy P, Winter PW, Wawrzusin P, York AG, Shroff H, Ramamurthi KS**. 2014. Asymmetric division and differential gene expression during a bacterial developmental program requires DivIVA. PLoS Genet. **10**:e1004526.

21. **Errington, J.** 1993. *Bacillus subtilis* sporulation: regulation of gene expression and control morphogenesis. Microbiol Rev. **57**:1-33.

22. **Errington J**. 2003. Regulation of endospore formation in *Bacillus subtilis*. Nat Rev Microbiol. **2**:117-126.

23. **Fimlaid KA, Shen A**. 2015. Diverse mechanisms regulate sporulation sigma factor activity in the Firmicutes. Curr Op Microbiol. **24**:88-95.

24. **Foster, S. J. and D. L. Popham.** 2002. Structure and synthesis of cell wall, spore cortex, teichoic acids, S-layers, and capsules, p. 21-41. *In* A. L. Sonenshein, J. A.

Hoch, and R. Losick (ed.), *Bacillus subtilis* and its closest relatives: from genes to cells. American Society for Microbiology, Washington, D.C.

25. **Fujita M, Gonzalez-Pastor JE, Losick R**. 2005 High- and low-threshold genes in the SpoOA regulon of *Bacillus subtilis*. J Bacteriol. **187**:1357–1368.

26. **Gerhardt P, Marquis RE**. 1989. Spore thermoresistance mechanisms, p 43–63. In Smith I, Slepecky RA, Setlow P (ed), Regulation of procaryotic development: structural and functional analysis of bacterial sporulation and germination. American Society for Microbiology, Washington, DC.

27. **Ghosh S, Scotland M, Setlow P**. 2012. Levels of germination proteins in dormant and superdormant spores of *Bacillus subtilis*. J Bacteriol. **194**:2221–2227.
28. **Ghosh S, Setlow B, Wahome PG, Cowan AE, Plomp M, Malkin AJ, Setlow P**. 2008. Characterization of spores of *Bacillus subtilis* that lack most coat layers. J Bacteriol. **190**:6741-6748.

29. **Gilmore ME, Bandyopadhyay D, Dean AM, Linnstaedt SD, Popham DL.** 2004. Production of muramic δ-lactam in *Bacillus subtilis* spore peptidoglycan. J Bacteriol. **186**:80-89.

30. **Griffiths KK, Zhang J, Cowan AE, Yu J, Setlow P**. 2011. Germination proteins in the inner membrane of dormant *Bacillus subtilis* spores colocalize in a discrete cluster. Mol Microbiol **81**:1061-1077.

31. **Henriques AO, Moran CP Jr**. 2000. Structure and assembly of the bacterial endospore coat. Methods. **20**:95–110.

32. **Henriques AO, Moran CP, Jr**. 2007. Structure, assembly, and function of the spore surface layers. Annu Rev Microbiol. **61**:555-588.

33. **Higgins D, Dworkin J.** 2012. Recent progress in *Bacillus subtilis* sporulation. FEMS Microbiol Rev. **36**:131-148.

34. **Hilbert, D. W. and P. J. Piggot.** 2004. Compartmentalization of gene expression during *Bacillus subtilis* spore formation. Microbiol Mol Biol Rev. **68**:234-262.

35. **Hornstra LM, de Vries, YP, de Vos, WM, Abee T**. 2006. Influence of sporulation medium composition on transcription of *ger* operons and the germination response of spores of *Bacillus cereus* ATCC 14579. Appl Environ Microbiol. **72**:3746–3749.

36. **Hudson KD, Corfe BM, Kemp EH, Feavers IM, Coote PJ, Moir A.** 2001. Localization of GerAA and GerAC germination proteins in the *Bacillus subtilis* spore. J Bacteriol. **183**:4317-4322.

37. **Igarashi T, Setlow B, Paidhungat M, Setlow P**. 2004. Analysis of the effects of a *gerF* (*lgt*) mutation on the germination of spores of *Bacillus subtilis*. J Bacteriol. **186**:2984–2991.

38. **Igarashi, T. and Setlow, P**. 2005. Interaction between individual protein components of the GerA and GerB nutrient receptors that trigger germination of *Bacillus subtilis* spores. J Bacteriol. **187**:2513–2518.

39. **Kaufmann R, Müller P, Hildenbrand G, Hausmann M, Cremer C.** 2010. Analysis of Her2/neu membrane protein clusters in different types of breast cancer cells using localization microscopy. J Microsc. **242**:46-54.

40. **Kim H, Hahn M, Grabowski P, McPherson DC, Otte MM, Wang R, Ferguson CC, Eichenberger P, Driks A.** 2006. The *Bacillus subtilis* spore coat protein interaction network. Mol Microbiol. **59**:487–502.

41. **Kong L, Doona CJ, Setlow P, Li YQ**. 2014 Monitoring rates and heterogeneity of high-pressure germination of *Bacillus* spores by phase-contrast microscopy of individual spores. Appl Environ Microbiol. **80**:345-353.

42. **Korza, G, Setlow, P**. 2013. Topology and accessibility of germination proteins in the *Bacillus subtilis* spore inner membrane. J Bacteriol. **195**:1484–1491.

43. **Kühlbrandt W**. 2014. Microscopy: Cryo-EM enters a new era. eLife. 3:e03678.

44. **Lewis PJ, Marston AL.** 1999. GFP vectors for controlled expression and dual labeling of protein fusions in *Bacillus subtilis*. Gene. **227**:101-109.

45. **Li Y, Davis A, Korza G, Zhang P, Li YQ, Setlow B, Setlow P.** 2012. Role of a SpoVA protein in dipicolinic acid uptake into developing spores of *Bacillus subtilis*. J Bacteriol. **194**:1875-1884.

46. **Li Y, Setlow B, Setlow P, Hao B.** 2010. Crystal structure of the GerBC component of a *Bacillus subtilis* spore germinant receptor. J Mol Biol. **402**:8-16.

47. **Li Y, Jin K, Gosh S, Carlson K, Devarakonda P, Davis A, Stewart KV, Cammett E, Pelczar-Rossi P, Setlow B, Lu M, Setlow P, Hao B.** 2014. Structural and functional analysis of the GerD spore germination protein of *Bacillus* species. J Mol Biol. **426**:1995-2008.

48. **Liang J, Zhang P, Setlow P, Li YQ**. 2014. High precision fitting measurements of the kinetics of size changes during germination of individual *Bacillus* spores. Appl Environ Microbiol. **80**:4606-4615.

49. **Luu S, Cruz-Mora J, Setlow B, Feeherry FE, Doona CJ, Setlow P**. 2015. The effects of heat activation on *Bacillus* spore germination, with nutrients or under high pressure, with or without various germination proteins. Appl Environ Microbiol. **81**:2927-2938.

50. **Lopez D, Vlamakis H, Kolter R**. 2009. Generation of multiple cell types in *Bacillus subtilis*. FEMS Microbiol Rev. **33**:152-163.

51. **Marquis KA, Burton BM, Nollmann M, Ptacin JL, Bustamante C, Ben-Yehuda S, Rudner DZ**. 2008. SpoIIIE strips proteins off the DNA during chromosome translocation. Genes Dev. **22**:1786-1795.

52. **Mason JM, Hackett RH, Setlow P**. 1988. Regulation of genes coding for small, acid-soluble proteins of *Bacillus subtilis* spores: studies using *lacZ* gene fusions. J Bacteriol. **170**:239-244.

53. **McKenney PT, Driks A, Eichenberger P**. 2013. The *Bacillus subtilis* endospore: assembly and functions of the multilayered coat. Nat Rev Microbiol. **11**:33–44.

54. **Molle V, Fujita M, Jensen ST, Eichenberger P, Gonzalez-Pastor JE, Liu JS, Losick R**. 2003 The SpoOA regulon of *Bacillus subtilis*. Mol Microbiol. **50**:1683–1701.

55. **Mongkolthanaruk W, Cooper GR, Mawer JSP, Allan RN, Moir A**. 2011. Effect of amino acid substitutions in the GerAA protein on the function of the alanine-responsive germinant receptor of *Bacillus subtilis* spores. J Bacteriol. **193**:2268 –2275.

56. **Nicholson WL, Setlow P**. 1990. Sporulation, germination and outgrowth, p. 391-450. *In* Harwood CR, Cutting SM (ed), Molecular biological methods for *Bacillus*. John Wiley and Sons, Chichester, England.

57. **Paidhungat M, Setlow P**. 1999. Isolation and characterization of mutations in *Bacillus subtilis* that allow spore germination in the novel germinant D-alanine. J Bacteriol. **181**:3341-3350.

58. **Paidhungat M, Setlow P**. 2000. Role of Ger proteins in nutrient and nonnutrient triggering of spore germination in *Bacillus subtilis*. J Bacteriol. 1**82**:2513- 2519.

59. **Paidhungat M, Setlow, P**. 2001. Localization of a germinant receptor protein (GerBA) to the inner membrane of *Bacillus subtilis* spores. J Bacteriol **183**:3982–3990.

60. **Paidhungat M, Ragkousi K, Setlow P**. 2001b. Genetic requirements for induction of germination of spores of *Bacillus subtilis* by Ca^{2+}-dipicolinate. J Bacteriol. **183**:4886-4893.

61. **Paidhungat M, Setlow P.** 2002. Spore germination and outgrowth, p. 537-548. *In* A. L. Sonenshein, J. A. Hoch, and R. Losick (ed.), *Bacillus subtilis* and its closest relatives: from genes to cells. American Society for Microbiology, Washington, D.C.

62. **Paredes-Sabja D, Setlow P, Sarker MR**. 2011. Germination of spores of Bacillales and Clostridiales species: mechanisms and proteins involved. Trends Microbiol. **19**:85–94.

63. **Pawson T, Scott JD**. 1997. Signaling through scaffold, anchoring, and adaptor proteins. Science. **278**:2075-2080.

64. **Pédelacq JD, Cabantous S, Tran T, Terwilliger TC, Waldo GS**. 2006. Engineering and characterization of a superfolder green fluorescent protein. Nat Biotechnol. **24**:79-88.

65. **Pelczar PL, Igarashi T, Setlow B, Setlow P**. 2007. Role of GerD in germination of *Bacillus subtilis* spores. J Bacteriol. **189**:1090–1098.

66. **Pelczar PL, Setlow P**. 2008. Localization of the germination protein GerD to the inner membrane in *Bacillus subtilis* spores. J Bacteriol. **190**:5635-5641.

67. **Peng L, Chen D, Setlow P, Li Y-q**. 2009. Elastic and inelastic light scattering from single bacterial spores in an optical trap allows the monitoring of spore germination dynamics. Anal Chem. **81**:4035–4042.

68. **Perez-Valdespino A, Li Y, Setlow B, Ghosh S, Pan D, Korza G, Feeherry FE, Doona CJ, Li Y-q, Hao B, Setlow P.** 2014. Properties and function of the SpoVAEa and SpoVAF proteins in *Bacillus subtilis* spores. J Bacteriol. **196**:2077-2088.

73. **Plomp, M, Leighton, TJ, Wheeler, KE, Hill, HD, Malkin, AJ**. (2007) In vitro high-resolution dynamics ofsingle germinating bacterial spores. Proc Natl Acad Sci USA. **104**:9644–9649.

74. **Popham DL, Helin J, Costello CE, Setlow P**. 1996. Muramic lactam in peptidoglycan of Bacillus subtilis spores is required for spore outgrowth but not for spore dehydration or heat resistance. Proc Natl Acad Sci USA. **93**:15405–15410.

75. **Ramirez-Peralta, A, Zhang, P, Li, YQ, Setlow, P**. 2012a. Effects of sporulation conditions on the germination and germination protein levels of spores of *Bacillus subtilis*. Appl Environ Microbiol. **78**:2689–2697.

76. **Ramirez-Peralta A, Stewart KA V. Thomas SK, Setlow B, Chen Z, Li YQ, Setlow P**. 2012b. Effects of the SpoVT regulatory protein on the germination and germination protein levels of spores of *Bacillus subtilis*. J Bacteriol. **194**:3417–3425.

77. **Regan G, Itaya M, Piggot P**. 2012. Coupling of sG activation to completion of engulfment during sporulation of *Bacillus subtilis* survives large perturbations to DNA translocation and replication. J Bacteriol. **194**:6264-6271

78. **Reymann J, Baddeley D, Gunkel M, Lemmer P, Stadter W, Jegou T, Rippe K, Cremer C, Birk U**. 2008. High-precision structural analysis of subnuclear complexes in fixed and live cells via spatially modulated illumination (SMI) microscopy. Chromosome Res. **16** (3): 367–82.

79. **Rodrigues CD, Marquis KA, Meisner J, Rudner DZ**. 2013. Peptidoglycan hydrolysis is required for assembly and activity of the transenvelope secretion complex during sporulation in *Bacillus subtilis*. Mol Microbiol. **89**:1039-1052.

80. **Setlow B, Cowan AE, Setlow P**. 2003. Germination of spores of *Bacillus subtilis* with dodecylamine. J Appl Microbiol. **95**:637-648.

81. **Setlow B, Setlow P**. 1996. Role of DNA repair in *Bacillus subtilis* spore resistance. J Bacteriol. **178**:3486-3495.

82. **Setlow B, Wahome PG, Setlow P**. 2008. Release of small molecules during germination of spores of *Bacillus* species. J Bacteriol. **190**:4759–4763.

83. **Setlow P.** 1988. Small, acid-soluble spore proteins of *Bacillus subtilis* species: structure, synthesis, genetics, function and their degradation. Annu Rev Microbiol. 42:319-338.

84. **Setlow P**. 2003. Spore germination. Curr Opinion Microbiol. **6**:550-556.

85. **Setlow P**. 2006. Spores of *Bacillus subtilis*: their resistance to and killing by radiation, heat and chemicals. J Appl Microbiol. **101**:514-525.

86. **Setlow P**. 2007. I will survive: DNA protection in bacterial spores. Trends Microbiol. **15**:172-180.

87. **Setlow P**. 2013. When the sleepers wake: the germination of spores of *Bacillus species*. J Appl. Microbiol. **115**:1251–1268.

88. **Setlow P**. 2014. The Germination of Spores of *Bacillus* Species: what we know and don't know. J Bacteriol. **7**:1297-1305.

89. **Setlow P, Liu J, Faeder JR**. 2012. Heterogeneity in bacterial spore populations, p 201–216. In Abel-Santos E (ed), Bacterial spores: current research and applications. Horizon Scientific Press, Norwich, United Kingdom.

90. **Shaner NC, Campbell RE, Steinbach PA, Giepmans BN, Palmer AE, Tsien RY**. 2004. Improved monomeric red, orange and yellow fluorescent proteins derived from *Discosoma* sp. red fluorescent protein. Nat Biotechnol. **22**:1567-1572.

91. **Steichen CT, Kearney JF, Turnbough, CL Jr**. 2007. Non-uniform assembly of the *Bacillus anthracis* exosporium and a bottle cap model for spore germination and outgrowth. Mol Microbiol. **64**:359–367.

92. **Stewart, Kerry-Ann.** 2014. Localization, quantitation, and interactions of germinant receptor proteins in the *Bacillus subtilis* spore inner membrane. *Doctoral Dissertations.* Paper 354. http://digitalcommons.uconn.edu/dissertations/354.

93. **Stewart, KA-V, Setlow P**. 2013. Numbers of individual nutrient germinant receptors and other germination proteins in spores of *Bacillus subtilis*. J Bacteriol. **195**:3575–3582l.

94. **Stewart K-AV, Yi X, Ghosh S, Setlow P.** 2012. Germination protein levels and rates of germination of spores of *Bacillus subtilis* with overexpressed or deleted genes encoding germination proteins. J Bacteriol. **194**:3156-3164.

95. **Sugawara E, Nagano K, Nikaido H**. 2012. Alternative folding pathways of the major porin OprF of *Pseudomonas aeruginosa*. FEBS J. **279**:910–918.

96. **Sugawara E, Nestorovich EM, Bezrnkov SM, Nakaido H**. 2006. *Pseudomonas aeruginosa* protein OprF exists in two different conformations. J. Biol. Chem. **281**:16220–16229.

97. **Sun DX, Cabrera-Martinez RM, Setlow P**. 1991. Control of transcription of the *Bacillus subtilis spoIIIG* gene, which codes for the forespore-specific transcription factor sigma G. J Bacteriol. **173**:2977-2984.

98. **Sun D, Stragier P, Setlow P**. 1989. Identification of a new sigma factor involved in compartmentalized gene expression during sporulation of *Bacillus subtilis*. Genes Dev. **3**:141–149.

99. **Sutcliffe IC, Harrington DJ**. 2002. Pattern searches for the identification of putative lipoprotein genes in Gram-positive bacterial genomes. Microbiology **148**:2065-2077.

100. **Tennen R, Setlow B, Davis KL, Loshon CA, Setlow P**. 2000. Mechanisms of killing of spores of *Bacillus subtilis* by iodine, glutaraldehyde and nitrous acid. J Appl Microbiol. **89**:330-338.

101. **Teruel M, Meyer T**. 2000. Translocation and reversible localization of signaling proteins: a dynamic future for signal transduction. Cell. **105**:181-184.

102. **Traag BA, Ramirez-Peralta A, Wang-Erickson AF, Setlow P, Losick R**. 2013. A novel RNA polymerase-binding protein controlling genes involved in spore germination in *Bacillus subtilis*. Mol Microbiol. **89**:113–122.

103. **Troiano AJ, Zhang J, Cowan AE, Yu J, Setlow P**. 2015. Analysis of the dynamics of a *Bacillus subtilis* spore germination protein complex during spore germination and outgrowth. J Bacteriol. **197**:252-261.

104. **Velasquez J, Schuurman-Wolters G, Birkner JP, Abee T, Poolman B.** 2014. *Bacillus subtilis* spore protein SpVAC functions as a mechanosensitive channel. Mol Microbiol. **92**:813-823.

105. **Velasquez-Gusman JC, Kocer A, Abee T, Poolman B**. 2012. SpoVA, putative channels involved in spore germination of *Bacillus* spores, abstr. 101. 5th Eur. Spores Conf., Egham, United Kingdom, 16 to 19 April 2012.

106. **Vepachedu VR, Setlow P**. 2007. Role of SpoVA proteins in release of dipicolinic acid during germination *of Bacillus subtilis* spores triggered by dodecylamine or lysozyme. J Bacteriol. **189**:1565–72.

107. **Wang ST, Setlow B, Conlon EM**, **Lyon JL, Imamrua D, Sato T, Setlow P,Losick R, Eichenberger P**. 2006. The forespore line of gene expression in *Bacillus subtilis*. J Mol Biol. **358**:16–37.

108. **Wang G, Yi X, Li YQ, Setlow P**. 2011. Germination of individual *Bacillus subtilis* spores with alterations in the GerD and SpoVA proteins, which are important in spore germination. J Bacteriol. **189**:4681-4687.

109. **Warth A**. 1978. Molecular structure of the bacterial spore. Adv Microb Physiol **17**:1-45.

110. **Wilson, M.J., Carlson, P.E., Janes, B.K. and Hanna, P.C**. 2012. Membrane topology of the *Bacillus anthracis* GerH germinant receptor proteins. J Bacteriol. **194**:1369–1377.

111. **Xiao Y, Francke C, Abee T, Wells-Bennik MH**. 2011. Clostridial spore germination versus bacilli: genome mining and current insights. Food Microbiol. **28**:266 –274.

112. **Yi X, Liu J, Faeder JR, Setlow P**. 2011. Synergism between different germinant receptors in the germination of *Bacillus subtilis* spores. J Bacteriol. **193**:4664-4671.

113. **Yi X, Setlow P**. 2010. Studies of the commitment step in the germination of spores of *Bacillus* species. J Bacteriol. **192**:3424 –3433.